HELLENIC REPUBLIC
National and Kapodistrian
University of Athens

Marine terraces of Kasos Island, Greece

Vasiliki Isouki
Supervising Professor: Niki Evelepidou,
Geology and Environment, NKUA
2023

Contents

1. Introduction

The island of Kasos, nestled in the mesmerizing Aegean Sea, is an intriguing location that offers a treasure trove of geological wonders and fascinating insights into the dynamic processes that have shaped its coastal landscapes. In this thesis, I will present a comprehensive study encompassing various aspects, including the classification and mapping of marine terraces, as well as an exploration of the island's geology, tectonics, and seismology.

Marine terraces, the focal point of this thesis, hold significant importance in understanding past sea-level changes and tectonic activities. In the following sections, we delve into the classification of marine terraces, examining their distinct characteristics and providing valuable insights into the processes that have influenced their formation.

To embark upon a comprehensive exploration, I begin by scrutinizing the geology of Kasos Island. By unraveling the geological composition, rock formations, and sedimentary history, I aim to unravel the island's geological evolution and gain a deeper understanding of the factors contributing to the development of marine terraces.

Tectonic processes have played a pivotal role in shaping the landscape of Kasos Island. Therefore, it is important to intricate tectonic framework, investigating the forces and mechanisms responsible for the island's structural deformation. Through an examination of fault systems, uplift patterns, and related tectonic features, the aim is to elucidate the tectonic history that has influenced the formation and preservation of marine terraces.

In addition, the seismology of Kasos Island has to be mentioned, as seismic activity often serves as a key indicator of ongoing tectonic processes. By analyzing seismic data and historical records, the aim to characterize the seismicity patterns of the island, offering valuable insights into the seismic hazards that have impacted its geological development and influenced the distribution of marine terraces.

The study culminates in a detailed investigation of the marine terraces in Kasos Island. Through meticulous mapping efforts, the goal is to provide a comprehensive overview of the distribution, extent, and characteristics of these landforms. The mapping results will be analyzed and interpreted in conjunction with the geological and tectonic context of the island, facilitating a deeper understanding of the factors contributing to the formation and preservation of marine terraces.

1.1 Marine terraces

Marine terraces are essential geomorphic features that may provide crucial information about palaeo-climate and surface deformation rates in coastal areas, in particular regarding vertical tectonic movements. Marine terraces are formed mostly during sea level highstand by the interaction between wave erosion and surface uplift. During highstands, wave erosion drives cliff retreat generating a rocky-shore platform etched on the landscape. Rocky-shore platforms are characterized by smooth and low sloping surfaces often covered by shallow marine deposits. Depending on the thickness of the sedimentary successions they can be divided into wave built and rocky-shore marine terraces. The wave-built marine terraces are gently sloping landforms formed

by thick accumulation of shallow marine sediments, whereas the rocky-shore marine terraces are landforms generated by wave erosion, comprising only a thin sedimentary cover. Marine terraces are usually abandoned during the following sea level lowstand period, if vertical displacements are faster and/or the next sea level highstand is lower than the previous one the platform can be preserved higher and safe from wave erosion.

In coastal areas, like the Mediterranean coast of the CAP southern margin, geomorphic features such as marine terraces represent the surface expression of combined tectonics and eustatic sea-level variations, providing detailed information about surface deformation during the Quaternary. Tectonic uplift is the main factor responsible for the preservation of marine terraces, forming staircase sequences in areas of rapid uplift rates (higher than 0,2 m/kyr). During periods of sea-level lowstand, marine platforms are abandoned, and new platforms can develop during sea level rise. At lower uplift rates, polygenetic marine terraces known as rasa surfaces can develop. These kinds of terraces are characterized by wide coastal plains bounded y steep cliffs, related to reoccupation during the successive sea-level highstands. Low uplift rates can also produce a total overprinting of older terraces, as demonstrated in some areas of the Mediterranean such Crete and southern Italy (Racano et al., 2020).

Marine terraces are an important element of coastal geomorphology. Their study had started by the1970s in several places of the world and has since expanded to almost all the coastal regions. The progress achieved is owed, to a great extent, to the development of accurate dating techniques and the establishment of the theory of the Pleistocene sea-level fluctuations. Given that marine terraces are the geological records of former sea levels, a steadily and rapidly rising coastline is the best mark for measuring major long term sea-level fluctuations and tectonic uplift. Their study could provide important information in dating fault activity and measuring rates of recent crustal deformation, which are very critical in establishing earthquake recurrence intervals, resolving the earthquake potential and evaluating the seismic hazard and risk. In Greece, marine terraces exist in various places such as on the southern coasts of the Gulf of Corinth and along several shores of the Hellenic arc, in the southern Peloponnese and in the islands of Kythera, Crete, Kasos, Karpathos and Rhodes. Marine terraces are excellent morphological markers and have been used world-wide to recognize past sea-level changes. An emerged marine terrace is a complex morphological feature, characterized by erosional and depositional elements. It is bounded landward by an inner edge representing the palaeoshoreline correlated to one of the main interglacial Oxygen Isotope Stages or Substages (OIS) ascribed by the global eustatic curve. The correlation of uplifted Quaternary marine terraces and palaeoshorelines with the main interglacial highstands can be done only in areas where significant geological and morphological evidence suggests the existence of a long-term continuous uplifting process at a regional scale, even though it is characterized by variable rates since the formation of the oldest marine terrace. The hypothesis that the mean uplift rate during the investigated time period is high enough to preserve the marine terraces, permitted the dating of the terrace sequence and the evaluation of the uplift history of raised coastal regions. The surface extension of the terraced surfaces depends on the duration of the sea-level stand, the erodibility of the local rock layers and the original morphology. In the Aegean area, these are preserved because of sufficient coastal uplift.
(Gaki-Papanastassiou et al., 2009).

In view of the existing problems, the geological analysis of the raised marine terraces can help in reconstructing Quaternary sea-level history. During Early Pleistocene-Middle Pleistocene, another Interglacial with a sea level probably lower than present MSL took place. The Interglacial is represented in uplifted trending areas by a wide marine terrace where several highstands are recorded (Zazo, 1999).

Raised paleoshorelines are among the best markers in the landscape for the assessment of the types and rates of geomorphic and tectonic processes. Worldwide, flights of marine terraces are used to constrain the amount and timing of vertical motions, one the glacio-hydro-isostatic component is removed from the modern vertical position of paleoshorelines. Due to their planar, subhorizontal geometry, marine terraces are also excellent markers of displacements along faults, thus providing first order constraints to the amount and chronology of fault activity eventually accompanying uplift of coastal areas. In fact, marine terraces may be short-lived landforms, more or less prone to be removed by erosion according to the combination of a number of factors. Flights of marine terraces testify to long-term Quaternary uplift in the order of several hundreds of meters of the horst of the southern Tyrrhenian margin (Cerrone et al., 2021).

Marine terraces are up to several kilometers in width in western Europe and other tectonically stable regions, and they can extend up to 200m or more in elevation. There are flights of elevated terraces, ranging up to 2 million years or more in age, along the steep hinterlands of the western coast of North America, and on other tentonically mobile coasts. These terraces were generally formed during the Quaternary, and they were elevated by tectonic uplift to their present positions. Whereas Tertiary terraces in tectonically stable regions developed along coasts that are imbedded in, or are situated along the trailing edge of, tectonic plates, Quaternary terraces have often developed on tectonically mobile coasts along plate boundaries (Trenhaile, 2002).

(a) The rate of erosion increases with the rate of rising and falling sea level although it may eventually decrease with very rapid changes in relative sea level.
(b) Terraces are formed during interglacial stages on rising landmasses, and during glacial stages on subsiding landmasses.
(c) Terraces preserve a more complete palaeo-sea level record on coasts that are rapidly rising or subsiding, than on coasts where changes in elevation are slow.
(d) The gradient of the terraces increased with tidal range, and they tended to be more gently sloping and wider in weaker rocks. The number of terraces increased with the rate of uplift and subsidence, and with the slope of the hinterland. Terraces tended to be narrower and more steeply sloping on steeply sloping landmasses.
(e) Inner edges are higher, relative to the tide, when the land is subsiding than when it is rising, and lower, relative to the tide, than contemporary cliff-platform junctions (Trenhaile, 2002).

The formation of marine terraces has intrigued for many years. In some areas of the world (such as in the vicinity of Hudson's Bay), terraces may be found high above the present water line and from this, the conclusion has been drawn that the sea at one time reached to where the terraces are located. Thus, there is some evidence that the present relative position of the sea and the land was not always as it is now. Changes of the relative position of these two media have been referred to as "eustatic changes".

The appearance of marine terraces has generally been taken as an indication that, during the eustatic changes, the surface of the sea remained at the level of the terrace for some time (May, 1993).

The Mediterranean Sea has a micro tidal range (< 0.3 m) and far-field wave energy is generally low. Nonetheless, marine terraces along coastal cliffs are extensive and often easily traced. Paleo-sea level indicators can be divided into sediment-poor and sediment-rich. Sediment-poor paleo-sea level indicators include notches, small sea caves, and sea arches that are formed by mechanical and bio-erosional processes. On Crete, and likely elsewhere in the Mediterranean, a distinct facies relationship exists between Pleistocene terraces and marine erosional features (Wegmann & Gallen, 2022).

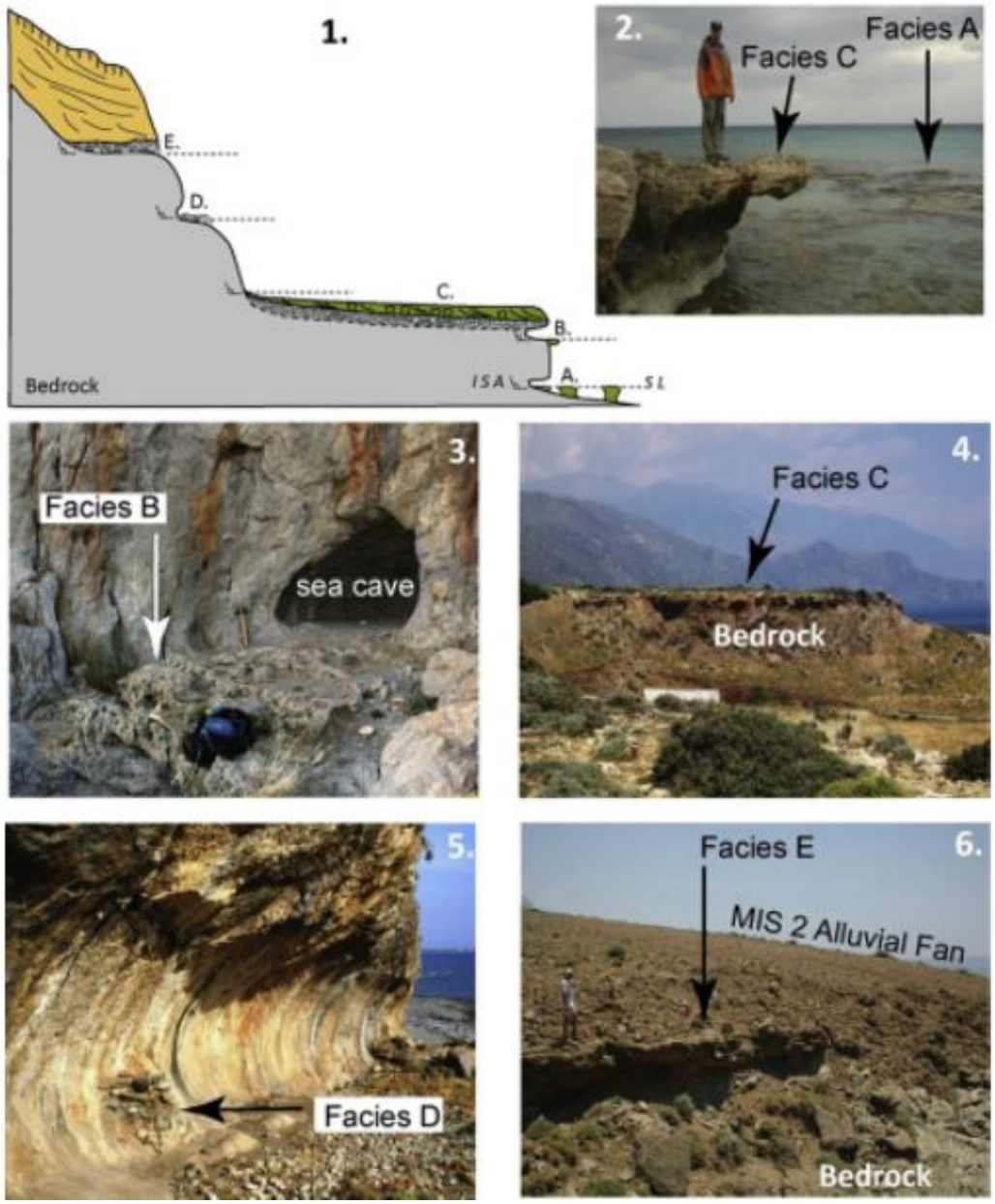

i (1) Idealized Pleistocene erosional and depositional terrace types (A–E) from western Crete with respect to relative sea level (SL) at the time of formation used to determine inner shoreline angle (ISA) elevations. The ordering of depicted stratig- raphy is for illustrative purposes. Five distinct sedimentological facies (A–E) are recognized and can be used to infer depositional environments and geomorphic setting. Facies designations are keyed to

photographs. Facies designations are keyed to photographs. (2) Facies A, modern algal bioherms and patch reefs. (3) Facies B, bioerosion notch with calcareous algae (Neogoniolithon sp.) and vermetid (Den- dropoma sp.) fringing reefs or trottoir associated with small sea cave, note hammer and blue backpack for scale. (4) Facies C—broad highstand calcareous algae and bryozoa bioherm reef with interstitial cemented bioclastic and siliciclastic sands developed above clastic transgressive cobble beach deposit, that in turn is beveled on steeply dipping sedimentary bedrock. The unconformity between the bedrock and marine terrace deposits is a seaward sloping planation surface (strath). (5) Facies D—clastic pebble-to-cobble beach deposit associated with wave-cut erosion notch etched into Mesozoic limestone bedrock; some bedrock erosion notches do not contain sediment lag. (6) Facies E—clastic cobble beach over bedrock planation surface, buried by younger seaward-prograding low-stand (e.g., marine isotope stage—MIS 2) alluvial fan deposits. Alluvial fan deposits have also been observed burying facies–C reefs.

Marine abrasion platforms, most commonly referred to as marine terraces, are erosional landforms that develop due to landward retreat of the active sea cliff in response to erosion by ocean wave energy, that may or may not have beach and marine deposits preserved on them. A marine terrace will develop whenever the rate of sea cliff retreat is significant compared to the rate of relative sea-level change so that a planar surface can be beveled onto the emerged coastline (Hisao Kondo et al., 2022).

Marine terraces are formed along the coastal zones of uplifting tectonic blocks. Block tilting is often observed with the formation of stepped terraces, inclined planation surfaces and vertical motions of coastlines. Marine abrasion platforms, which when uplifted are referred to as marine terraces, are erosional landforms that develop due to landward retreat of the active sea cliff in response to erosion by ocean wave energy. A marine terrace will develop whenever the rate of sea cliff retreat is significant compared with the rate of relative sea-level change so that a planar surface can be beveled onto the continent margin (H. Kondo & Owen, 2013).

A marine terrace is any relatively flat surface of marine origin, bounded by a steeper ascending slope on one side and by a steeper descending slope on the opposite side. Marine terraces may result from marine abrasion or denudation (marine-cut terraces, or shore platforms, see Figure 5), or consist of shallow water to slightly emerged accumulations of materials removed by shore erosion (marine-built terraces), or also have a polygenic origin, with occurrence of in situ deposits after an abrasion phase (Figure 11). The occurrence of a series of stepped marine terraces usually results from eustatic changes in sea level superimposed on a tectonic trend. Uplifted terraces that act as a continuous tape recorder, each step developing when the rising sea level overtakes the rising land, may be most useful for Quaternary environmental studies, since each terrace can be considered as a fossil counterpart of the present-day terrace, platform, or reef flat. In seismic areas, however, terrace steps may have a tectonic origin (Pirazzoli, 2013).

Marine terraces are wave-cut surfaces formed especially during sea level highstands that are often mantled with a layer of sand (Granger & Riebe, 2014).

A marine terrace is an almost flat surface of marine origin. They can be shaped by marine erosion and can consist of shallow water to slightly emerged accumulations of materials redistributed by shore erosional and depositional processes. (Rovere et al., 2016). The occurrence of a flight of marine terraces in a coastal region is the result of the interaction between long-term tectonic uplift and Quaternary cyclic sea-level fluctuation, associated with global climatic changes (Karymbalis et al., 2022). Due to their particular morphology, marine terraces are used for sea level studies, especially those adressing coastal uplift. Moreover, they can be used for paleoreconstruction of

the environment and are important indicators of paleo sea level changes (Rovere et al., 2016).

Figure 2 *A wide, flat marine terrace extends for many kilometers east of Chah Bahar, Iran, especially between Beris (photo) and the Pakistani border. Source: https://www.sciencedirect.com/topics/earth-and-planetary-sciences/marine-terrace*

Figure 3 *Uplifted terrace in Wellington. Source: https://www.geotrips.org.nz/trip.html?id=693*

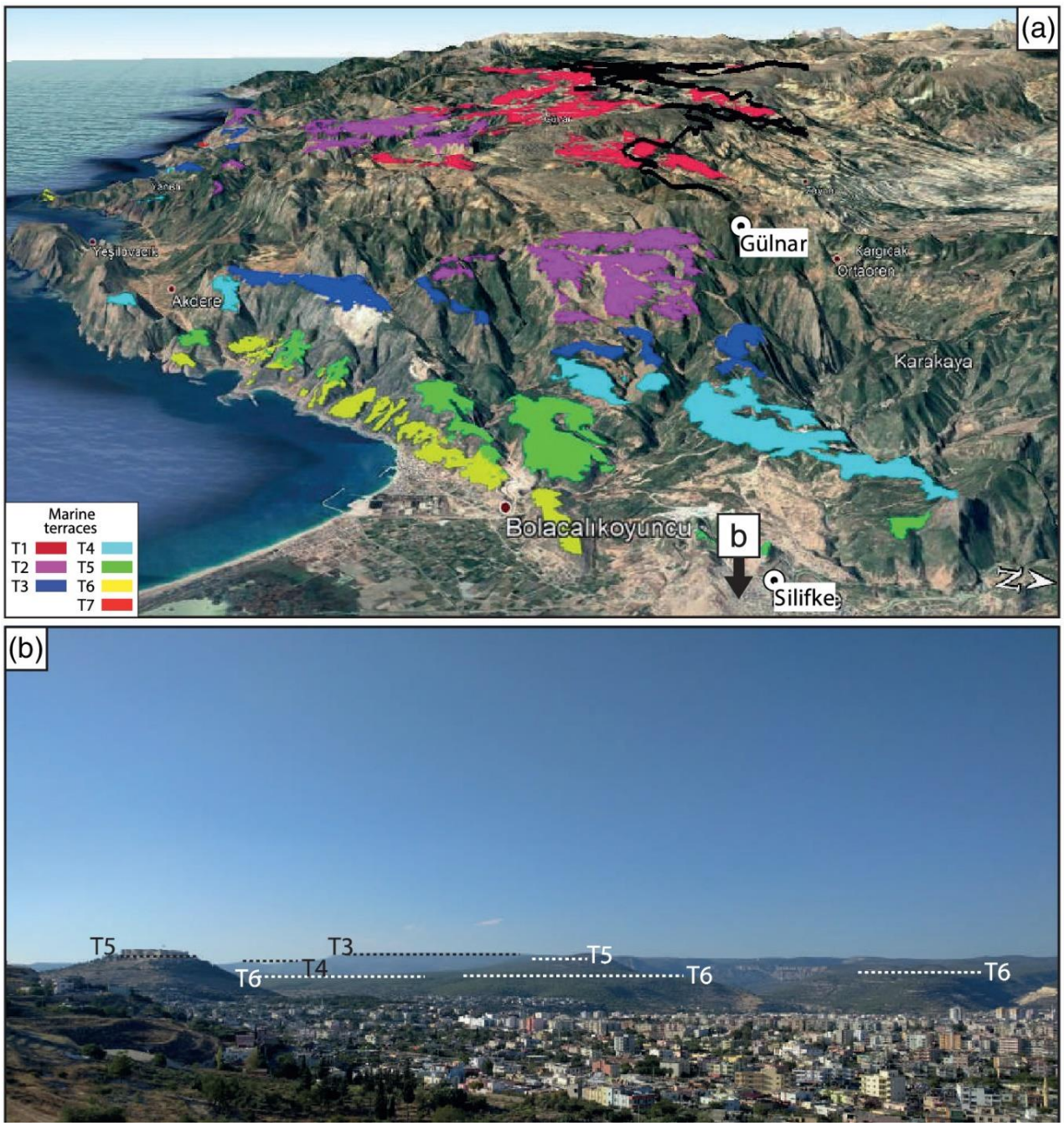

Figure 4 *Google Earth picture of the staircase sequence of marine terraces from the top of the polateau margin toward the sea (a) and panoramic of marine terraces in the area of Silifke (b)* (Racano et al., 2020)

A marine terrace is any flat, horizontal, or slightly sloping surface of water that's bounded by a steeper ascending or descending slope on one side and a steeper descending slope on the other (May, 1993). Its slope varies from 1-5 degrees depending on the tidal range of the area. A marine terrace can rise up to 600 meters above the present sea level, but in the Mediterranean the most developed terraces are probably those of Tunisia with a height of 400 meters (Evelpidou, 2020). They are most commonly observed in regions that are tectonically uplifting and are though to form during periods of relative sea-level stability and are abandoned following sea-level highstands (Karymbalis et al., 2022).

In temperate regions, these types of surfaces are usually caused by marine erosion. Usually, these surfaces are formed from the shallow-water accumulations of sand and other materials that were removed from the shore by the erosion. In tropical regions, bioconstruction can occur due to the accumulation of reef materials (May, 1993).

The development of elevated marine terraces usually correlates with the superimposition of tectonic and eustatic changes in the sea level. These types of surfaces are also known as continuous tape recorders. As the rising sea level moves toward the land, these terraces will continue to develop. Each raised terrace, eventually capped by marine and/or alluvial materials, is a fossil counterpart of the present- day terrace, platform, or reef flat. For relatively rapid uplift rates (e.g., >1 mm/yr), each marine terrace corresponds to a different interglacial period or stage and ages usually increase with elevation, with the uppermost levels being the less well-preserved since they are exposed longer to the erosional processes. For slower uplift rates, marine terraces may have a polycyclic origin, sea level returning again at the terrace level after a period of exposure to weathering. When reconstructing past sea-level changes from the study of datable raised marine terraces, two assumptions are usually made: (1) that the eustatic sea-level position corresponding to at least one raised terrace is known and (2) that the uplift rate has remained essentially constant in each section. From these assumptions, the eustatic sea level can be calculated for each dated terrace (May, 1993).

A marine terrace typically consists of two distinct surfaces: an abrasion ramp dipping gently seaward and an inland-bounding sea-cliff dipping seaward. The junction between the roughly flat paleo-platform and its internal palaeo-cliff is called the palaeoshoreline angle (also called the inner edge of the platform), and it is here that a wave-cut notch may be preserved. The inner edge represents a marker that closely approximates the elevation of the local sea level at the time of terrace formation, typically during sea-level highstands. On flights of terraces where only one terrace can be dated, steady uplift is often assumed, and the altitudinal spacing of the terraces is used to assign sea-level highstand ages (Karymbalis et al., 2022).

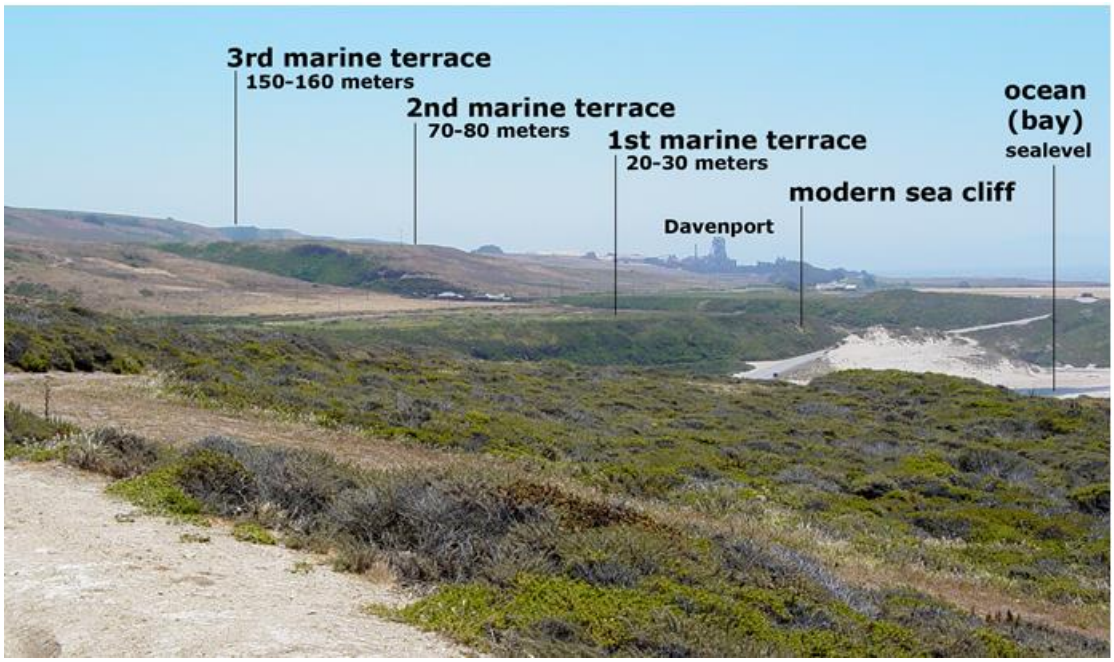

Figure 5 *Marine terraces at Davenport, California. Source: https://gotbooks.miracosta.edu/geology/chapter12.html*

Figure 6 *Google Earth image looking north at a wave-cut platform and marine terrace, Cape Blanco, Oregon. Source: https://www.sciencedirect.com/topics/earth-and-planetary-sciences/wave-cut-platform*

1.2 Classification of marine terraces

Marine terraces can be classified into two types based on their geomorphic characteristics: emergent and submerged (Gurrola et al., 2014; Bilbao-Lasa et al., 2020).

1. Emergent marine terraces

Emergent marine terraces are formed by tectonic uplift of the coast, where the land is raised above the sea level. These terraces are located at a higher elevation than the present shoreline and can be several meters above the current sea level. Emergent marine terraces are formed by a combination of tectonic uplift, sea level changes, and wave erosion. These terraces have a gentle slope and a flat surface that is parallel to the current shoreline. Emergent marine terraces are an important indicator of tectonic activity in the coastal region and they can be used to reconstruct the timing and magnitude of past earthquakes and tsunamis (Howell et al., 2015; Gurrola et al., 2014).

2. Submerged marine terraces

Submerged marine terraces are formed by a rise in sea level. These terraces are located below the present shoreline and can be several meters below the current sea level. Submerged marine terraces are formed by a combination of sea level rise, wave erosion, and sediment deposition. These terraces have a gentle slope and a flat surface that is parallel to the current shoreline. Submerged marine terraces are an important indicator of sea level changes in the coastal region (Bilbao-Lasa et al., 2020).

Ricchi et al. (2018) has provided new insights into marine terrace development on reefless volcanic islands. used high-resolution marine geophysical data offshore Santa Maria Island in the Azores Archipelago to investigate the formation of marine terraces. They found that marine terraces on reefless volcanic islands develop differently from those on continental shelves, with wave erosion playing a more important role. These findings have important implications for understanding past sea level changes and predicting future coastal erosion on similar island systems.

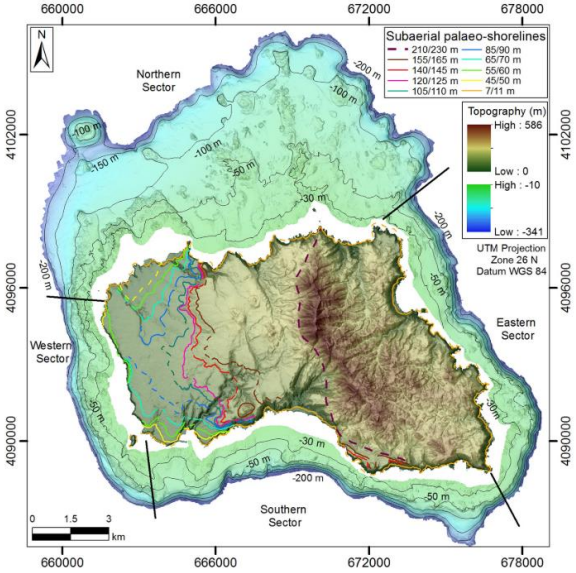

Figure 7 *Shaded relief map of the subaerial part of Santa Maria Island and surrounding shelf (derived from the multibeam bathymetry). Black lines represent the limits of the Northern, Western, Southern and Eastern sectors described in the text. Colored solid and dashed lines represent the location of the evident and inferred inner margins of subaerial marine terraces. (For interpretation of the references to colour in this figure legend, the reader is referred to the web version of this article.)(Ricchi et al., 2018).*

The classification of marine terraces based on their elevation is an essential tool for understanding the geological history of coastal regions. It provides information on the relative sea level changes that have occurred over time, and it allows for the identification of terraces that formed during different sea-level highstands. The classification scheme also helps to understand the age of the marine terraces, with higher terraces being older than lower ones.

Intermediate-level marine terraces are those found between the high and low marine terraces. These terraces are usually less developed than high and low terraces, and their morphology is more variable. Intermediate-level marine terraces are found between 10 and 200 meters above sea level and represent a range of sea levels that existed during the past few hundred thousand years. These terraces are important in sea-level studies because they record multiple sea-level fluctuations within the Quaternary period (Athanassas & Fountoulis, 2013).

Low-level marine terraces are those located at or just above the present sea level. They represent the most recent marine transgression and are usually less developed than older terraces. Low-level marine terraces are also referred to as the Holocene terraces, and they are characterized by the presence of wave-cut notches and small beach ridges. The Holocene terraces are important in sea-level studies because they provide information on the rate and timing of sea-level change during the last several thousand years (Athanassas & Fountoulis, 2013).

1.3 Materials and Methods

1.3.1. Mapping - examples

To carry out the analysis of the marine terraces, detailed field surveying, mapping, sampling and outcrop description are required (Nandy et al., 2021). The first step is the detailed mapping of the distinct marine terrace surfaces and their inner edges (the palaeoshoreline angle of each palaeo-platform). Mapping, usually is carried out using both Geographic Information System (GIS) and field techniques such as aerial photography and sampling. A GIS spatial geodatabase must be created using as primary data a Digital Elevation Model (DEM), topographic and geological maps along with secondary layers such as terrain roughness and slope (Karymbalis et al., 2022; Tsanakas et al., 2022). All of the above must be supported by extensive field investigations (Karymbalis et al., 2022).

For instance, Tsanakas et al., 2022 using GIS procedures with extensive field work identified 7 (I-VII) uplifted marine terraces along the southern coast of the Cephalonia Island. Their spatial distribution as well as their description can be shown in the following Figure:

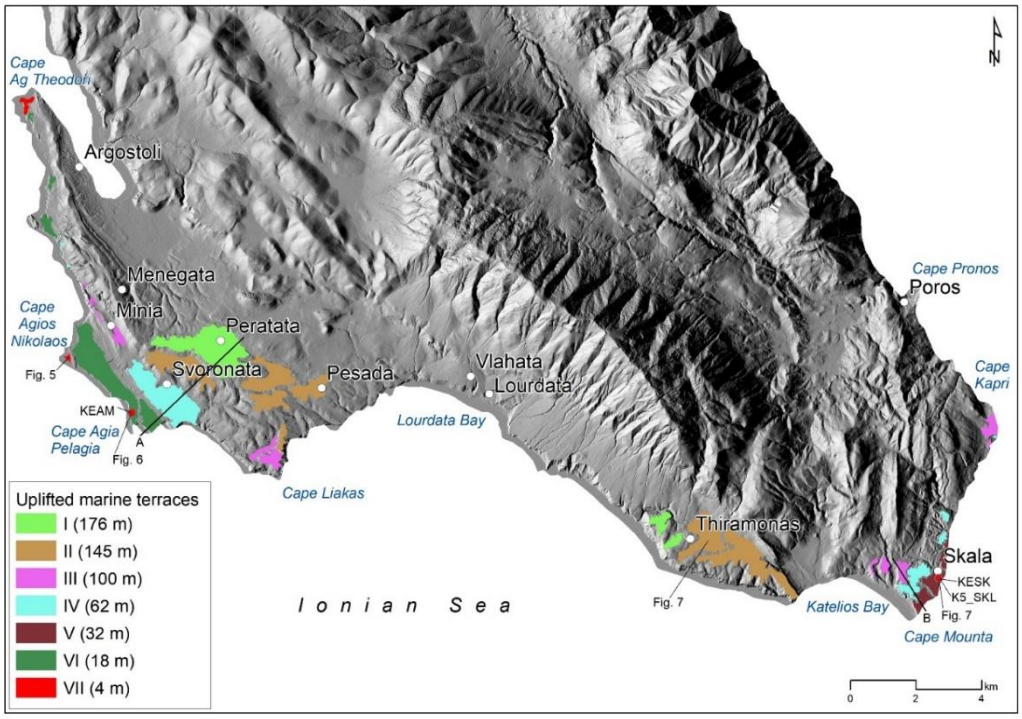

Figure 7 *Spatial distribution of the prominent uplifted marine (Tsanakas et al., 2022)*

Another example of similar method of mapping can be shown from Karymbalis et al., 2022 in the area of Neapolis, where they identified 10 uplifted marine terraces along the coastline between cape Koulendi and Agia Marina, west of cape Maleas. Furthermore, the marine terraces flight, consisting of 10 emerged abrasion platforms, can be traced with shoreline angles on Elafonissos Island. The final detailed map of those marine terraces can be shown in the following Figure:

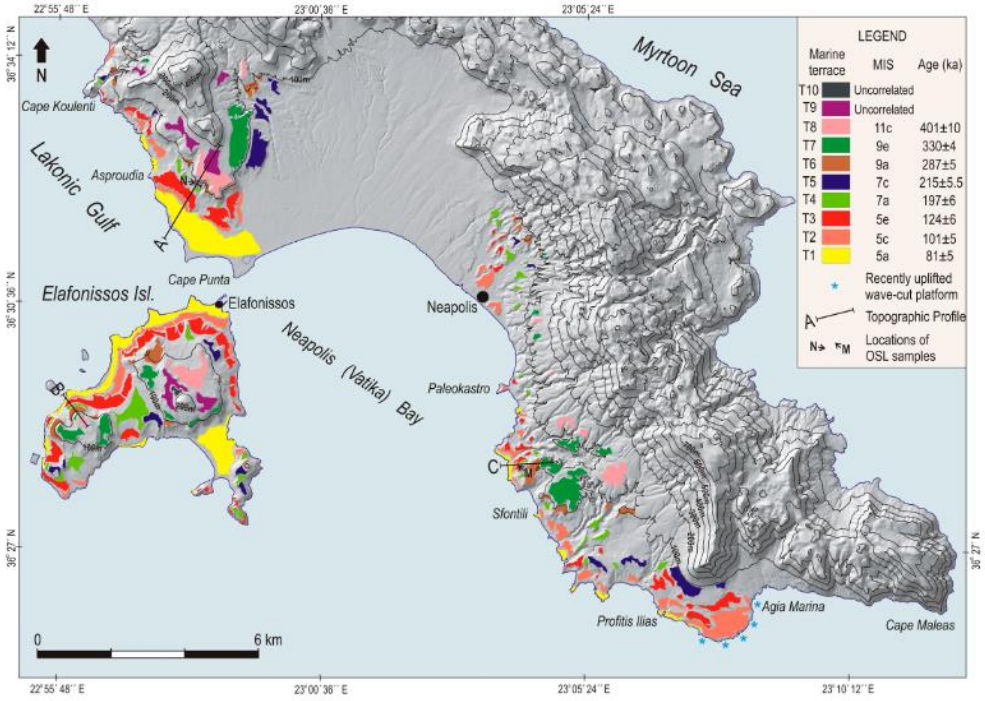

Figure 8 *Geographic distribution of the uplifted marine terraces of the broader Neapolis area, southeastern Peloponnese (Karymbalis et al., 2022)*

1.3.2. Dating Methods

Understanding the evolution of coastal landscapes and unraveling the intricate tapestry of past sea-level changes and tectonic processes is a fundamental pursuit in geology and Earth sciences. Marine terraces, prominent landforms associated with former shorelines, offer valuable insights into the dynamic interplay between sea-level fluctuations and crustal movements. To decipher the chronological framework of these terraces and reconstruct the geological history of coastal regions, it has been employed a range of dating methods. This chapter delves into the diverse techniques utilized to determine the ages of marine terraces, including radiocarbon dating, optically stimulated luminescence (OSL) dating, cosmogenic nuclide surface exposure dating, and uplift rate analysis. Each method provides a unique window into the past, enabling scientists to piece together the complex puzzle of coastal evolution.

Radiocarbon Dating: Radiocarbon dating, a cornerstone technique in archaeology and geochronology, relies on the radioactive decay of carbon-14 (^{14}C) isotopes in organic material. By analyzing the ratio of stable carbon isotopes (^{12}C and ^{13}C) to ^{14}C in samples extracted from marine terrace sediments, it can be estimated the age of the organic matter and, by extension, the associated terrace. This method is particularly effective for dating relatively young terraces spanning the late Holocene, providing essential chronological constraints for coastal research.

Optically Stimulated Luminescence (OSL) Dating: OSL dating offers a powerful tool for determining the ages of sediment grains deposited on marine terraces. It measures the time elapsed since these grains were last exposed to sunlight or heat, thereby resetting their luminescence signals. By analyzing luminescence emissions from minerals such as quartz and potassium feldspar, OSL dating provides approximate ages for marine terraces. This technique is especially pertinent for studying Pleistocene terraces, shedding light on past sea-level changes and tectonic uplift in coastal regions.

Cosmogenic Nuclide Surface Exposure Dating: Cosmogenic nuclide surface exposure dating provides a unique perspective on the age of marine terraces by assessing the accumulation of cosmogenic isotopes, such as beryllium-10 (^{10}Be) and aluminum-26 (^{26}Al), in exposed rock surfaces. By measuring the isotopic concentrations, it can be estimated the duration of terrace exposure to cosmic radiation, allowing them to determine the terrace's age. This method is particularly valuable for studying older terraces that experienced long periods of surface exposure.

Uplift Rate Analysis: In addition to dating techniques, uplift rate analysis plays a crucial role in deciphering the formation and evolution of marine terraces. By quantifying the vertical displacement of terraces relative to sea level, it can be inferred the rates at which tectonic uplift or subsidence has occurred over geological timescales. This information provides critical insights into the dynamic nature of coastal landscapes and the processes shaping them.

By integrating these diverse dating methods and uplift rate analysis, it can be constructed robust chronologies of marine terraces, revealing the temporal patterns of sea-level changes and tectonic activities. These investigations contribute to a deeper understanding of Earth's coastal history, unraveling the complex interplay between geodynamic processes and environmental change. As we delve into the intricacies of

each dating technique, we unravel the secrets of marine terraces, gaining valuable insights into the dynamic nature of our planet's coastal realms.

1.3.2.1 Optically Stimulated Luminescence (OSL) Dating

Optically stimulated luminescence (OSL) dating provides a measure of time since sediment grains were deposited and shielded from further light or heat exposure, effectively resetting the luminescence signal. This dating method relies on measuring the luminescence emitted by specific minerals, commonly quartz or potassium feldspar, when stimulated by light (Tanaka et al., 1997). OSL dating is particularly relevant in studying Pleistocene terraces, which are landforms associated with former shorelines. These terraces provide valuable insights into past sea-level changes and tectonic uplift (González-Acebrón et al., 2016).

By analyzing sediment samples collected from these terraces and applying OSL dating techniques, it can be determined the approximate ages of these landforms. For example, Karympalis et al. (2022) conducted a study on a series of ten uplifted terraces representing former shorelines. In their research, they collected samples from two different terraces and utilized OSL dating to estimate their ages. The obtained results revealed that the first terrace had an age of approximately 121.7 thousand years (ka), while the second terrace was dated to be around 218.8 ka.

Another example of dating marine terraces using OSL dating was conducted by Tanaka et al. (1997). For the OSL measurements, they employed an Elsec Type 9010 Automated Optical Dating Reader. Stimulation was conducted using 500±40 nm light, which was carefully selected by optical filters from the output of a 150 W halogen lamp. To detect the ultraviolet luminescence, specific emission filters (such as Hoya U340 and Scott UGI l) were utilized in conjunction with an EMI 9235Q photomultiplier.

To ensure accurate measurements, the samples underwent a normalization process. This involved subjecting the samples to a short exposure (approximately 0-5 mJ) of natural light, followed by artificial irradiation using a $^{90}Sr/^{90}Y$ source with a dose rate of 4 Gy/min. Prior to the OSL measurement, the samples underwent pre-heating for 5 minutes at 220°C.

The OSL emissions detected from these samples were typically characterized by low intensity and exhibited significant disc-to-disc scatter. These characteristics can pose challenges during data analysis and interpretation. However, by carefully analyzing and comparing the additive dose OSL shine curves obtained from marine terrace sediment samples, it can be derived valuable insights into the luminescence properties and dating potential of these sediments.

The utilization of specific equipment and techniques in the OSL measurement process, such as the automated optical dating reader, precise light stimulation, and photomultiplier detection, ensures the reliability and accuracy of the obtained OSL data. By analyzing the luminescence emissions from these sediments, it can be extracted

valuable chronological information and contribute to our understanding of the geological history and evolution of marine terrace formations.

These findings, along with the research conducted by González-Acebrón et al. (2016), highlight the significance of OSL dating in understanding the chronology of Pleistocene terraces and their relationship to sea-level fluctuations and tectonic processes. By accurately determining the ages of these landforms, they can reconstruct the geological history of coastal regions and gain insights into past environmental changes.

The application of OSL dating to Pleistocene terraces is just one example of how this method contributes to our understanding of Earth's past. OSL dating has also been utilized in various other contexts, such as dating archaeological sites, examining sediment deposition patterns, and reconstructing climatic changes. Its ability to provide chronological information based on luminescence signals has made it a valuable tool in geochronology and paleoenvironmental research.

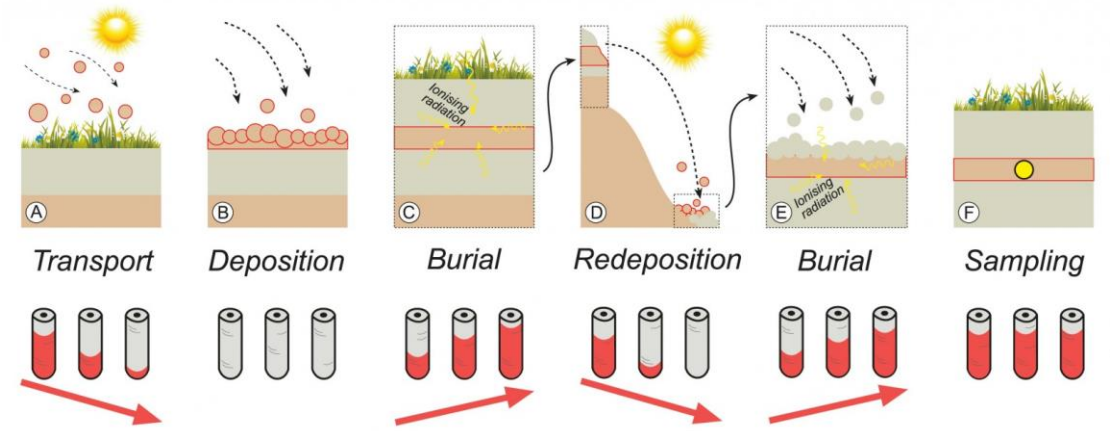

Figure 9 *Accumulation and release of charge within mineral grains (modified from Duller, 2008). (A) During transport of sediment the accumulated charge gets released due to energy provided by natural sunlight; (B) At deposition, the charge is fully released and the "battery" is emptied; (C) Charge can accumulate within the grain during burial due to natural ionising radiation; (D) and (E) The process described before can happen multiple times over geological times scales, depending on the environment and the geological processes; (F) When a sample is taken in opaque tubes or using cores the stored energy at that particular time gets sampled and can later be released in the laboratory to obtain a luminescence age. Source: https://blogs.egu.eu/divisions/cl/2018/09/03/how-glowing-sediment-can-help-to-decipher-the-earths-past-climate/*

Figure 10 *A laboratory model of the combined TL/OSL ready developed by Risø National Laboratory. Source: https://sci.esa.int/web/sci-fmp/-/40503-optically-stimulated-luminescence-dating-osl*

1.3.2.2 Carbon-14 (14C) Dating or radiocarbon dating

Carbon-14 dating is an isotopic method based on the radioactive decay of ^{14}C into ^{14}N. It is usually used to date Holocene and interglacial terraces.

^{14}C is created because N^{14} atoms interact with cosmic rays to form carbon-14, which is unstable. This isotope of carbon, which is absorbed by all organisms on Earth, decays radioactively and has a half-life of 5,730 years. So, because the ^{14}C atoms quickly combine with the oxygen in the atmosphere they create carbon dioxide, which in turn combines with the rest of the CO_2 in the atmosphere. This is absorbed by the oceans and organisms and through the food chain, they return to animals and plants. The radioactive carbon seen in animal organisms reflects the radioactive C in the atmosphere. This happens because, living organisms may lose ^{14}C at a constant rate due to radioactive decay, but at the same time renew it from the atmosphere due to constant interaction. So when organisms die, because ^{14}C has a specific half-life, we can calculate based on its percentage, the age of the organism.

However, the variation of ^{14}C over time is not constant for various reasons, either due to cosmic radiation, climate change, etc. For this reason, the ages calculated by the lab were younger than the real ones because the current ^{14}C ratio, which is not stable, was used for dating. To solve this problem, calibration is applied. Essentially, to be able to correct ages, tree-dating is applied to tree rings, with simultaneous ^{14}C dating and Uranium-Fluorine dating. Using these methods it has been possible to construct specific curves and software that can be used to calibrate the samples. Essentially, the older the sample's age, the greater the difference from its true age will be.

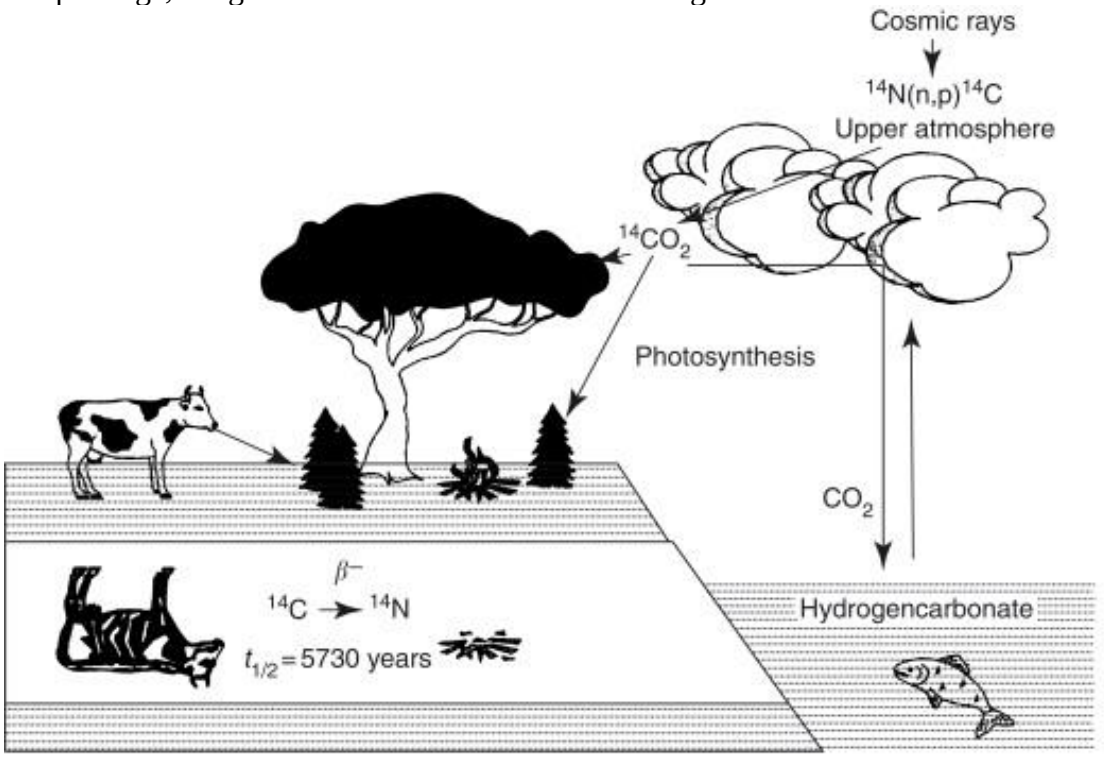

Figure 11 *Schematic depiction of the 14C cycle. Source: https://www.sciencedirect.com/topics/medicine-and-dentistry/radiometric-dating*

1.3.2.3 Cosmogenic Nuclide Surface Exposure Dating

This method relies on the measurement of isotopes, such as ^{10}Be and ^{26}Al, which are produced by the interaction of cosmic rays with rock at the Earth's surface. The production rate of these isotopes is known to vary with altitude, latitude, and depth (Kim & Sutherland, 2004).

In the study conducted by Kim & Sutherland (2004) in southwestern Fiordland, they used ^{10}Be and ^{26}Al apparent exposure ages to determine the age of uplifted granite bedrock surfaces and large boulders that were created by coastal erosion and subsequently modified by various geological processes. The objective was to investigate the age of coastal erosion in this setting and assess the influence of isotope inheritance and uncertainties associated with later surface modifications (Kim & Sutherland, 2004).

Cosmic rays interact with the atmosphere, ocean, and rock, leading to the production of secondary particles and the formation of cosmogenic nuclides. Neutron spallation is the primary mechanism for producing these nuclides in quartz up to a depth of 3-4 meters. The production rate decreases exponentially with depth, and at around 42 cm depth, the production rate is halved compared to the surface production rate. Muon interaction continues to produce ^{10}Be and ^{26}Al deeper into the rock, making it significant in cases of high denudation rate or accelerating denudation rate (Kim & Sutherland, 2004).

The ratio of ^{26}Al/^{10}Be can provide insights into the influence of deep production or prolonged shielding by overlying material, which may lead to lower ratios than the surface production rate. Measuring both isotopes allows to assess the significance of inherited ^{10}Be and ^{26}Al over different timescales, with a ratio close to that of surface production indicating minimal inheritance over shorter timescales (Kim & Sutherland, 2004).

By analyzing the apparent exposure ages of the samples and considering the geomorphic arguments, Kim & Sutherland, (2004)were able to determine the age of terrace formation and uplift rates associated with coastal erosion in the study area (Kim & Sutherland, 2004).

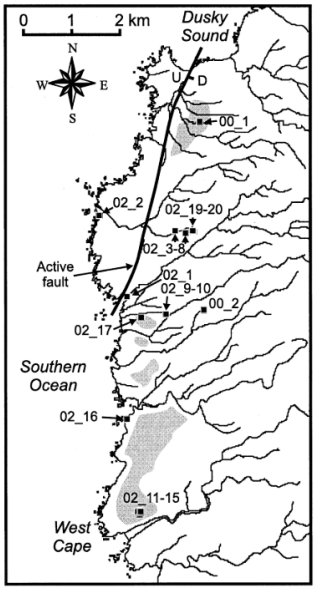

Figure 12 *Map of the study area displaying rivers, coastlines, and sampling sites. The coastal regions are where the three sea level sampling locations of 02_1, 02_2, and 02_16 can be found. The colored sections display the size of the marine terrace with the strandline at 65 meters above sea level. In these shaded areas, our low terrace (51–72 m) samples were collected. The samples in the open areas to the right of the shorelines are all collected on the upper terrace, which is 92–136 meters above sea level. In the northern portion of the region, a noticeable active fault is upthrown to the west (upthrown/downthrown sides are denoted U/D) (Kim & Sutherland, 2004).*

1.3.2.4 Uplift rates

Tsanakas et al., 2022 took three main parameters into consideration in order to estimate the uplift rate. These parameters included the absolute elevation of an uplifted marine terrace (which should normally correspond to the elevation of the inner edge of the terrace), the age of the formation of the respective terrace and the elevation of the sea-level in respect to the present day sea-level according to the following equation:

$$U=\frac{(Z-SL)}{T}$$

Where U: Uplift rate, Z: absolute elevation of the marine terrace, SL: Sea-level at the time of formation of the terrace and T: Age of the terrace.

Although the above equation includes all the necessary parameters to calculate an uplift rate, does not take into account the errors, on the eustatic sea-level curve. Therefore, they used a sea-level curve to estimate a minimum and a maximum uplift using a modified version of the above equation, aiming to first calculate the total uplift of the marine terrace and by dividing by the age of the terrace, to obtain the uplift rate U:

$$U_{min} = \frac{(Z - SL_{max})}{T_{max}}$$

$$U_{max} = \frac{(Z - SL_{min})}{T_{min}}$$

1.2. Kasos island

Kasos Island, located in the southernmost part of the Dodecanese archipelago, is situated approximately 6 kilometers west-southwest of Karpathos and 45 kilometers east-northeast of Cavo Sidero, the easternmost promontory of Crete (Melas, 1984). It is part of the natural island passage that connects Crete with southwestern Asia Minor, along with Karpathos, Saría, and Rhodes islands. Kasos is a mountainous and challenging island, with several distinct mountain ranges distributed across its terrain. It is surrounded by a group of islands and islets. The largest group, known as the Kasonisia, lies opposite the northern coast (Mastropavlos, 2019). Spanning a length of 17 kilometers in an almost NE-SW direction and measuring 8 kilometers in width, Kasos covers an area of 66.41 km^2, or 69 km^2 when including the small islands to the north (Armathia and Macronisi) (Melas, 1984; Athanassiadis, 2000; Cattaneo & Grano, 2021).

Additionally, the largest island, Armathia, with an area of 2567 km^2 and a maximum altitude of 111 meters, located northwest of Kasos, and the smallest, Porioni, with an area of 21 km^2, situated between the islands of Armathia and Makronisi (Cattaneo & Grano, 2021).The island consists mainly of high limestone masses, forming mountain ranges. The highest peak in northeastern Kasos is Megalos Priwnas, reaching an elevation of 601 meters (Athanassiadis, 2000).

Figure 13 *The Location of Kasos Island Source: Google Earth*

Figure 14 *Kasos Island Source: Google Earth*

Characterized by its mountainous and rugged terrain, particularly in the southeast and southwest regions, the island slopes towards the northwest where most of the modern settlements are concentrated. Mount Kapsalo, with an elevation of approximately 956 meters, dominates the central part of the island, while Mount Megalos Priwnas rises to 601 meters on the eastern side. Armathia Island, a partially submerged ridge, runs parallel to the north coast of Kasos (Melas, 1984; Athanassiadis, 2000).

The shores of Kasos mainly consist of high and rocky cliffs, with deep waters close to the coastline. The northeast coast is deeply indented with torrent beds that descend into small, steep coves. In contrast, the south coast is precipitous, while the western half, although still rugged, features slightly lower cliffs. The more cultivable and less rocky section is found in the northwest, traversing the fertile valley of Argos, which has softer soil and faces northeast but is also accessible from the northwest. This lowland area encompasses most of the arable land on the island (Melas, 1984).

Historical records indicate that Kasos had forests in ancient times, as evidenced by the presence of poor pasture and remnants of scrub in the western part of the island. It is known that during the Turkish occupation and the War of Greek Independence, shipbuilding took place in Kasos using timber imported from Karpathos and other sources. This suggests that the island likely had an ample supply of timber in ancient times (Melas, 1984).

While Kasos does not have perennial streams or springs, the island relies on wells to provide water, although it is often brackish. Rain-cisterns also contribute to the water supply (Melas, 1984).

The island of Kasos is characterized by its rugged and inaccessible coastlines, marked by deep gorges that terminate in small coves. The northern side of Kasos offers

the most accessible stretch of coastline, extending from Fry to Antiperatos. On the southwestern coast, the only bays present are Helatros and Avlaki (Cattaneo & Grano, 2021). In terms of natural harbors, the north coast features the port of Fri, situated at the head of a small open bay and protected from northwest winds by a rocky promontory. However, landing in this area can be challenging during northerly winds. Moving eastward from Fri, Yalos bay consists of an open beach that stretches to Emborio, where anchorage and a landing place can be found. Additional anchorages can be found off Amoua, east of Capy Saint George, and in Khelatros bay, which is considered the best harbor on Kasos (Melas, 1984).

Moreover, there are sheltered sandy beaches near the islets located to the north of Kasos, offering protection from northwesterly winds. Among these beaches, the most favorable anchorage is found off the central part of the elongated flat islet Makra, situated at the northeastern end of the group . These landing places, although currently deemed inconvenient, would have provided ancient vessels with shelter as they were drawn up the shore, particularly during the winter months (Melas, 1984).

3. Geology of Kasos island

All the islands in the western external orogenic arc of the Hellenic region, including Kasos, exhibit a comparable geological succession associated with the Alpine evolution (Mascle et al., 1986). Kasos island is characterized by a single, jagged ridge composed of durable limestone. This ridge extends from east to west and then turns towards the northwest and northeast (Melas, 1984). Geologically, Kasos is part of this arc, which encompasses the Pindos, Peloponnese, Crete, and the Dodecanese. The island is characterized by three distinct geological layers that were formed at different times and contain a variety of metallic elements (Mastropavlos, 2019).

The oldest layer, situated at the core of the island, predates the Cretaceous period and consists of crystalline rocks, schist, and marble. The middle layer, which spans the entire island and shapes its terrain, is predominantly composed of compact limestone and was formed between the Mesozoic-Cretaceous and Neogene periods. Lastly, the uppermost layer, originating during the Miocene and Pliocene epochs, consists of marl and thin layers of fine-grained limestone. Limestone and sandstone are the primary rock types found on the island (Mastropavlos, 2019).

The geology of Kasos is defined by eight formations that showcase its diverse geological history. The first formation, the Semimetamorphic Series of Peloponnese - Crete, dates back to the Jurassic to Eocene period and consists of undivided "platy" limestones series (Plattenkalk). The Gavrovo - Tripolis Zone, originating from the Mesozoic to Eocene ages, includes: a) black dolomites with pyrite (Upper Triassic) directly thrust over the Ionian zone, b) a chert succession where marl-sandstone beds alternate with small-scale lenticular limestone of Priabonian age, and c) gypsums associated with the tectonic contacts and the chert mentioned above. The Post-Tectonic and Late-Tectonic Sediments can be further divided into three zones: m3, which represents Upper Miocene lacustrine deposits with detrital sediments and local lignite beds; mp, consisting of Mio-Pliocene marine deposits with detrital sediments and occasional gypsum beds; and mq1, comprising Pleistocene marine deposits including marls, clays, sands, conglomerates, coastal terraces, and "porous" formations of

Cycledes islands. The cq1 zone encompasses Pleistocene lacustrine and continental deposits such as clays, loam, sands, conglomerates, and red clayey material, with travertine present in the Veria and Edessa areas. Finally, the Al zone represents Holocene alluvial deposits found in valleys, plains, and coastal areas (Melas, 1984; Athanassiadis, 2000; Kokkalas & Doutsos, 2001; Geological Survey of Greece, 2022).

Neogene sediments (Al)

The Neogene and Quaternary sediments of Kasos island are unconformably placed on top of the Alpine bedrocks of the basement and they are scattered almost throughout the surface of the island (Athanassiadis, 2000). However, the main areas of their development are:

a) the Neogene basin extents from Antiperatos beach, Arvanitochori to Poli region,
b) the area of Trita beach in the southerneast and
c) near the area of Saint Charalampos Skafis

Pleistocene (cq1, mq1)

The Pleistocene formations are present in various regions such as Agios Ioannis, Armathia islet etc. They are characterized by marine deposits consisting of detrital sediments and occasional gypsum beds. Typically, there is an absence of red clayey material. Additionally, brackish facies deposits are occasionally found in this area (Geological Survey of Greece, 2022).

The Lower Pleistocene in the Agios Ioannis basin consists of both marine and terrestrial formations, with particularly clastic characteristics and lateral and vertical lithological variations even over short distances. Lithologically, these formations comprise white or blue marls and clays, yellow sandy marls (predominant in the southern and southeastern parts of the basin), white tabular marly limestones, calcareous marls, friable brown sands, sandstones, calcarenites, and chalky conglomerates. Lithofacially, they represent deposits of closed or shallow seas (marls, clays, sandy marls, tabular marly limestones), coastal deposits (sandstones and cohesive chalky conglomerates), deltaic deposits (sandy marls and chalky conglomerates), and margin deposits (chalky conglomerates) (Athanassiadis, 2000).

Their Lower Pleistocene age is evidenced by the fossils found so far, including microfauna such as Globorotalia puncticulata, G. bononieusis, and G. aemiliana (Upper Taviano and Lower Piakenzian) and the NN15 nanofossil zone (Lower Pleistocene). Additionally, the accumulation of foraminiferal shells in the tabular marly limestones and calcareous marls is noteworthy. Barrier (1979) identified fossils of the Pecten species Adunctus and Dukneri, as well as nanofossils of the Lower Pleistocene or even older ages in the central part of the Agios Ioannis basin. Based on this observation, it suggests that a portion of the formations in the central basin may belong to the Upper Miocene. In the southeastern part of the basin, specifically, the beds of tabular marly limestones dip towards the southeast (Athanassiadis, 2000).

Mio-Pliocene (Upper Miocene – Pliocene) (mp)

This formation is found exclusively in the southeastern part of Kasos Island, spanning between the regions of Saint George and Saint Charalampos Skafis. It primarily consists of marine deposits, including detrital sediments and occasional

gypsum beds. Typically, there is an absence of red clayey material, although brackish facies deposits may be present as well (Geological Survey of Greece, 2022).

Miocene (m_3)

The Miocene formations on Kasos Island consist of both marine and terrestrial deposits, with an average total thickness of approximately 250 meters. Lithologically, these formations comprise a variety of sediment types, including marls, sandy marls, marly limestones, bio-calcarenites, sandstones, conglomeratic sandstones, and conglomerates. The conglomerates contain loosely connected, lightly rounded calcareous clasts ranging in size from a few centimeters to a few tenths of a meter, embedded within a red clayey matrix (Athanassiadis, 2000).

From a lithofacies perspective, these deposits represent different environments: coastal deposits characterized by sandstones and cross-bedded conglomeratic sandstones, deep-sea and shallow marine deposits composed of sandy marls, marls, biomicrite, and marly limestones, and fluvial deposits consisting of conglomeratic sandstones with a red clayey matrix (Athanassiadis, 2000).

The Upper Miocene age of these deposits is supported by the presence of various fossils, including fracture-breccias such as Pecten praebenedictus, Pecten revolutus, Chlamys solarium, Chlamys spinulosa, Crassostrea, Cardium spondyloides, and scaphopods like Dentalium novemcostatum mutibile. Microfossils, including Neolveolina melo, Miliolidae, Rotalidae, and Elpidium sp., further confirm their Upper Miocene age. Interestingly, no Neogene sediments younger than the Upper Miocene have been identified on Kasos, indicating that the upper part of the Kasos Neogene sequence represents a marine circle of Upper Miocene deposits. This marine transgression occurred on a pre-Upper Miocene paleo-relief. The sequence itself begins with a thick breccia with red argillaceous cement, which fills the pre-Upper Miocene basins. Subsequently, marly-sandy phases develop, transitioning upwards to predominantly allochthonous limestone that forms outside of these basins (Athanassiadis, 2000).

The oldest layers (je and ft) found on the island date back to the Pre-Cretaceous period and consist of continental crystalline rocks, schists, and marbles. These layers are primarily exposed in the central part of the major folded structures. The soils covering these rocks are sandy and light, lacking fertility except in well-watered areas. Due to their iron-rich weathering and water-retaining capacity, these areas are densely vegetated, typically with evergreen scrub vegetation, which has persisted despite centuries of poor management. They offer limited grazing opportunities and are sparsely cultivated or inhabited. Woodcutting, goat-keeping, and occasionally beekeeping have been the main occupations in these regions. The valleys within these formations contain more fertile soil washed down from the hillsides. Most of the island's mineral resources are found in these deposits (Melas, 1984).

Above these ancient layers lie upper Mesozoic-Cretaceous and Eocene strata, indicated as the "Me formation" in the geological map. These bulky rocks consist of massive limestone, exhibiting significant thickness and intense folding. They have undergone dislocation during subsequent mountain-building events, when the Alpine, Dinaric, and Tauric mountain systems experienced major uplift. As a result, these rocks have been subjected to continuous weathering. They extensively cover the island, as shown in the accompanying figure. The compact limestone beds range in color from

light yellow to pink, with a few lithographic flagstone layers that contain fossilized remains of unknown age. Some areas also contain deposits of serpentine associated with these rocks (Melas, 1984).

These limestone formations shape the island's morphology and give rise to distinctive "karst" landscapes characterized by surface erosion and the formation of caves and sinkholes. The soil cover is minimal, and the exposed surface is often barren and arid. Rainfall infiltrates through the porous limestone, leading to the formation of underground channels and caves that drain water to lower levels, including underwater springs. The limestone districts are typically devoid of water sources, resulting in limited vegetation, poor grazing conditions, and sparse human population (Melas, 1984).

The subsequent deposits found on the islands, although not significant in terms of geological structure, play a crucial role in their ecological functioning. These deposits consist of Tertiary marls and thin-bedded limestone layers that overlay the older, massive limestone formations (Melas, 1984). They were formed during the initial movements of mountain-building in the Miocene and Pleistocene periods within the mountainous region, specifically during the lower part of Upper Messinian (Melas, 1984; Kokkalas & Doutsos, 2001). As a result of the folding of mountain ridges, troughs were created, and the Mediterranean Sea extended far into these mountainous areas. In some regions, inland drainage led to the formation of freshwater lakes that occasionally evaporated, leaving behind gypsum and freshwater marl deposits. Additionally, deposits from coastal areas contributed to filling the troughs, alternating with subsequent layers of relatively pure limestone that formed during periods of greater subsidence (Melas, 1984).

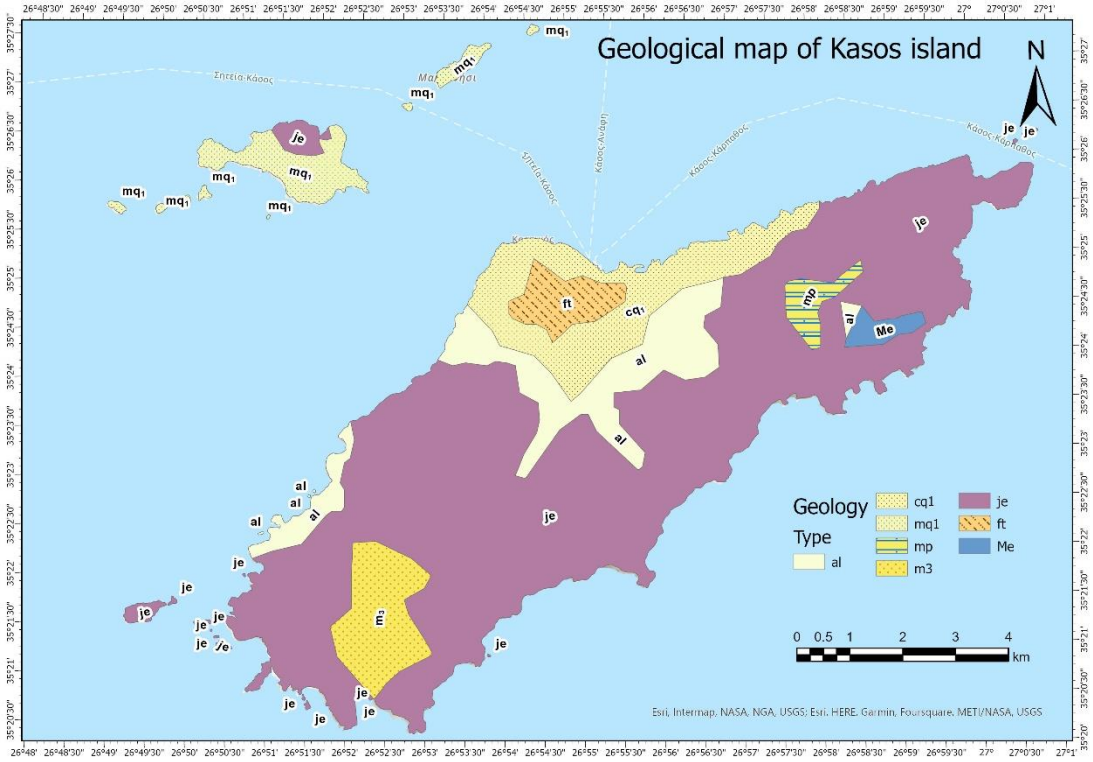

Figure 15 *The geological map of Kasos Island Source: Geological Survey of Greece, 2022*

4. Tectonics of Kasos island

The Hellenic Arc, also known as the Aegean Arc, serves as the boundary between the relatively narrow and slightly deformed Mediterranean Basin and the highly deformed allochthonous Hellenic mountain ranges. Compared to other island arcs worldwide, such as those in the Caribbean, Indonesia, and Japan, the Hellenic Arc is relatively small. It exhibits typical island arc characteristics and is composed of several distinct segments, including the Hellenic Trench, the Mediterranean Ridge, an outer sedimentary arc (encompassing Kythira, Antikythira, Crete, Kasos, Karpathos, and Rhodes), the marine basin of the southern Aegean Sea (Cretan Sea), and an inner volcanic arc (including Aegina, Milos, Santorini, and Nisyros) (Athanassiadis, 2000).

The eastern Hellenic margin can be divided into three main sectors based on morphology. The first sector comprises the continental margin and adjacent trenches southeast of Crete, the second sector includes the continental margin and trench stretching from Kasos to southern Rhodes, and the third sector consists of the continental margin and trough southeast of Rhodes (Mascle et al., 1986).

The geological history of the Aegean region has been shaped by three significant events that created dispersal barriers. Firstly, the formation of the mid-Aegean trench (MAT) led to the separation of Crete from the Karpathos island complex around 12 million years ago (Mya). During the Tortonian period (around 8 Mya), the Karpathos island group became isolated but was later integrated with the continents during the Messinian period (5-5 Mya). The Karpathos island complex joined Rhodes and Anatolia in the Lower Pliocene, but separation occurred around 3.5 Mya. Finally, Kasos detached from Karpathos approximately 10,000 years ago, during the late Pleistocene. Kasos is situated on the eastern boundary of the South Aegean Island Arc, connecting the Balkans to the Anatolian mainland. The island primarily consists of Mesozoic and Paleogene limestones, with some marine Neogene deposits covering parts of the lowlands. Quaternary deposits, such as piedmont screes and alluvions, can be found in the northern and western regions of the island, along with localized karst deposits (Cattaneo & Grano, 2021).

Large-scale normal faulting has played a significant role in shaping the morphology of the southern Aegean region during the late Neogene and Quaternary periods. The fault systems exhibit different orientations in various parts of the arc. Oblique NNW-SSE, N-S, and NNE-SSW fault systems are prominent in the Kythira-Antikythira strait to the west, while NE-SW faults dominate in the Kasos-Karpathos strait to the east. These fault systems are primarily characterized as pure normal faults, with some exhibiting dextral or sinistral displacements (Angelier et al., 1982).

Although compression forces have been observed in specific areas, the neotectonic evolution of the Hellenic arc is mainly driven by extensional processes associated with large-scale normal faulting. Consequently, the uplift of the arc cannot be solely attributed to lithospheric compression (Angelier et al., 1982).

The Karpathos-Kasos area exhibits two distinct directions of submarine morphology. The northern and central parts of Karpathos display an NW-SE direction, while the southern parts of Karpathos and Kasos exhibit an NE-SW direction. These

directions are indicative of a succession of tectonic subsidence and uplift, reflecting the riftogenic tectonics in the two islands (Athanassiadis, 2000).

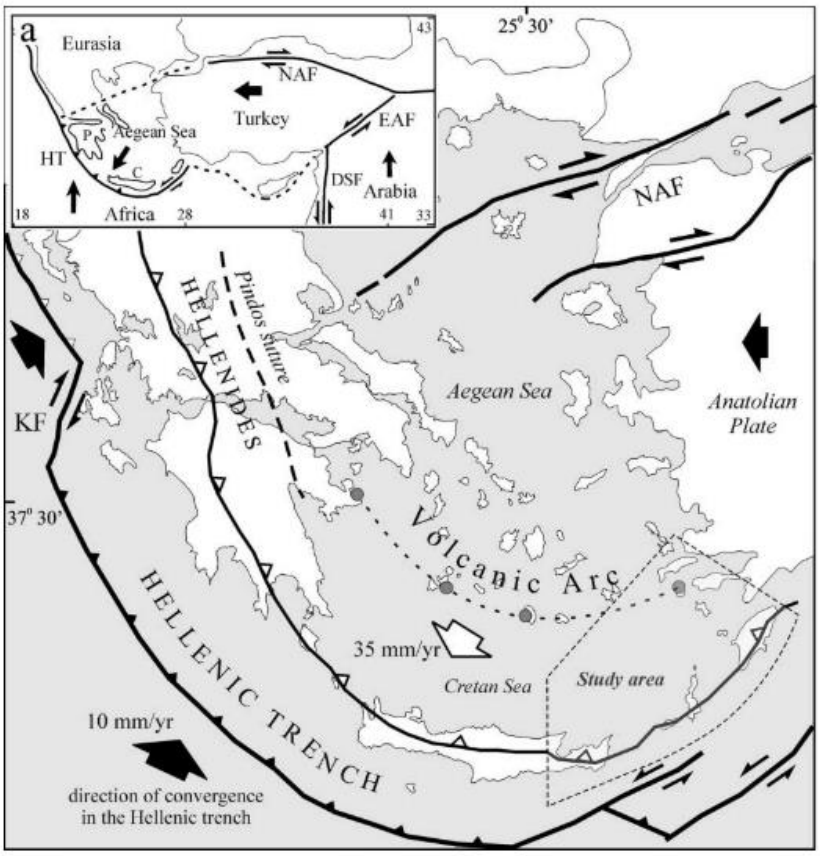

Figure 16 *(a) A simplified depiction of the primary structural characteristics of the Hellenic Arc and Trench system. Key fault abbreviations include: KF: Kefallonia Fault, NAF: North Anatolian Fault. Inset a: A schematic map providing an overview of the geodynamic framework in the eastern Mediterranean, illustrating the major plates involved in the collision process. Key abbreviations are as follows: NAF: North Anatolian Fault, EAF: East Anatolian Fault, DSF: Dead Sea Fault, HT: Hellenic Trench, P: Peloponnese, C: Crete* (Kokkalas & Doutsos, 2001).

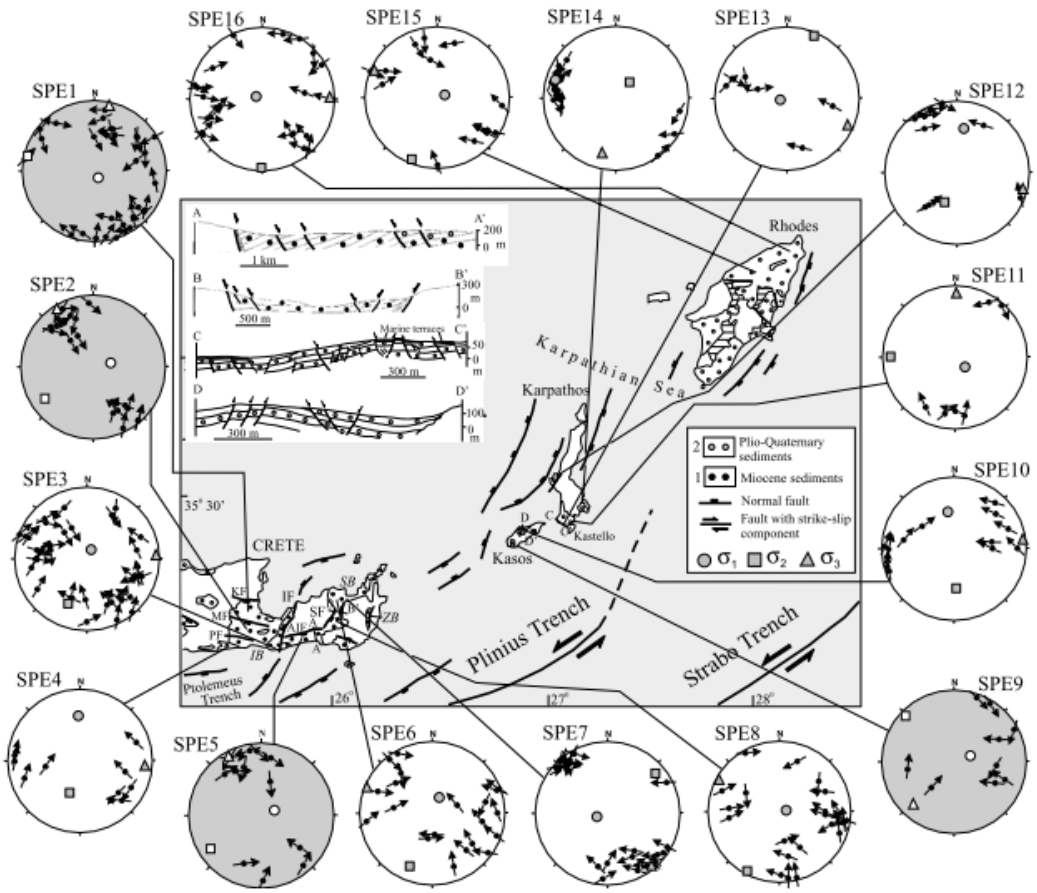

Figure 17 *A simplified map showcasing the southeastern Aegean region. Key features and abbreviations include: IB: Ierapetra basin, SB: Sitia basin, ZB: Zakros basin, AIF: Agios Ioannis Fault, KF: Kritsa Fault, IF: Ierapetra Fault, SF: Sitia Fault, MF: Makrilia Fault, PF: Parathiri Fault* (Doutsos & Kokkalas, 2001)

In Kasos island, two areas were studied: the area of Antiperatos, west of Fry, and the area of Megalos Priwnas in northeastern Kasos. These areas exhibit tectonic activity characterized by normal faults with directions of ENE-WSW and SE-SW, respectively. The faults have steeply dipping reflective surfaces covered by loosely to moderately consolidated breccia debris. The deposits in these areas, particularly those with alternations, indicate the activation of faults and subsequent processes (Athanassiadis, 2000).

The examination of terrestrial deposits along the northeastern coast of Kasos reveals significant indications and evidence of tectonic activity during the Upper Pleistocene. The calcarenites in this area were formed by accumulations of aeolian deposits, indicating alternating periods of tectonic activity and tectonic quiescence. These terrestrial deposits are affected by a NE-SW trending fault and exhibit typical extensional structures associated with a normal fault of NE-SW orientation (Athanassiadis, 2000).

On the southwest coast of the islet of Armathia and around Moucheli Bay in Kasos, a significant Tyrrhenian uplift ranging from 10m to 29m in elevation has been observed. This uplift is correlated with the rich fauna, indicating a Tyrrhenian uplift of the Castello Cape in Karpathos with an age of 260,000 years (Athanassiadis, 2000).

Kasos and Armathia have been gradually uplifting from the Upper Pliocene-Lower Pleistocene to the Upper Pleistocene. The average uplift rates for the coastlines of

Kasos were calculated to be 2.24 cm per century, 3.3 cm per century, and 1.9 cm per century for the paleoshorelines of 260,000 years, 120,000 years, and 80,000 years, respectively. Additionally, it was determined that for a period of approximately 740,000 years (between 1,000,000 and 260,000 years), the average uplift rate of the coastlines of northern and central Karpathos and Kasos was approximately 4.41 cm per century. The average uplift rate of the coastlines of Karpathos and Kasos during the Lower and Middle Pleistocene is approximately twice as high on average compared to the corresponding uplift rate during the Upper Pleistocene (Athanassiadis, 2000).

These findings indicate a complex tectonic evolution in Kasos, with periods of rapid uplift, tectonic stability, and significant sea-level fluctuations induced by climatic changes. The geological features and uplift rates provide valuable insights into the tectonic history and geodynamic processes that have shaped Kasos Island during the Pleistocene (Athanassiadis, 2000).

4.1 Tectonic evolution of Kasos Island

The geotectonic evolution of Kasos Island can be divided into different periods:

Paleogene

During the Paleogene period, which occurred approximately 66 to 23 million years ago, tectonic events associated with the opening of the Aegean Sea and the collision between the African and Eurasian plates shaped the geological framework of the region. These processes led to the formation of the Alpine basement, which consists of various geotectonic units such as ophiolitic melange, flysch, limestone, and marl formations. These early tectonic activities set the stage for subsequent geotectonic events and the evolution of Kasos Island (Athanassiadis, 2000).

Early to Middle Miocene

In the early to middle Miocene, roughly 23 to 11 million years ago, the Karpathos-Kasos region experienced extensional tectonic forces. These forces caused the formation of normal faults oriented in a general north-south direction. As a result, the tectonic units in the region became fragmented and displaced. This extensional tectonic regime also led to the development of grabens and half-grabens, where sedimentary deposits accumulated. The tectonic activity during this period played a crucial role in shaping the initial basin configuration and subsequent tectonic events in the region (Athanassiadis, 2000).

Middle to Upper Miocene

Continuing into the middle to upper Miocene, approximately 11 to 5 million years ago, the tectonic activity in the Karpathos-Kasos region intensified. Major faults with north-south and east-west orientations affected the area. These tectonic forces created folds with a general north-south direction, resulting in the folding and thrusting of the upper tectonic units. The deformation phase was followed by compressive tangential forces acting from the northwest, which led to the southward thrusting of the upper tectonic units onto the lower tectonic unit composed of "placoid limestones." Significant tectonic events, including metamorphism, folding, anticlinal uplift, and

fragmentation through normal faults, occurred during this time interval (Athanassiadis, 2000).

Sea level variations during the Holocene, which began approximately 11,700 years ago and continues to the present, have played a crucial role in shaping the tectonic evolution of the Karpathos-Kasos region. The study of vertical movements and tectonic deformations along the coasts of Kasos during the Holocene provides evidence of sea level changes. Submerged paleo-shorelines, erosion surfaces, coastal lithosome formations, and coastal archaeological structures indicate significant fluctuations in sea level. The coasts of Kasos have experienced subsidence, with an estimated average subsidence of 1-1.5 meters from the Roman period to the present and around 3.5-4 meters from the Minoan period to the present. These sea level variations have contributed to the morphotectonic characteristics of Kasos, shaping its present-day morphology through erosion by waves, rainfall, and water currents (Athanassiadis, 2000).

Upper Miocene to the present

During the Upper Miocene, the sea invaded the tectonic depressions of Kasos, possibly under tectonic control, and covered the entire island. The major marine transgression reached its peak during the Lower Quaternary, followed by a regression in the recent Pleistocene. The presence of fault orientations in multiple directions suggests polydirectional extension rather than distinct activations. Tectonic basins surrounding Kasos indicate tectonic activity in the region, likely with an age predating the Pleistocene. The study of vertical movements and tectonic deformations along the coasts of Kasos during the Holocene reveals evidence of sea level changes and tectonic subsidence. Submerged paleo-shorelines and archaeological structures indicate vertical movements and subsidence of Kasos' shores over the past millennia (Athanassiadis, 2000).

Furthermore, based on mammal fossils found on Kassos Island, it is suggested that Kassos and Karpathos were connected during the Lower-Middle Pleistocene period (Dermitzakis & Triantaphyllou, 1990).

In summary, Kasos Island has undergone complex geotectonic processes over different geological periods, including extension, folding, thrusting, uplift, subsidence, and the formation of faults. These processes, combined with sea level variations during the Holocene, have shaped the island's geological and morphological characteristics, creating a diverse and dynamic geological history (Athanassiadis, 2000).

4.2. Morphotectonics

The morphology of a region, both on the seabed and on the surface, including features such as relief, karst formations, hydrographic network, sediment structure, erosional surfaces, sinkholes, and wave erosion, is greatly influenced by its tectonic condition. By studying and observing the geomorphology of an area, we can indirectly draw conclusions about its tectonic condition (Athanassiadis, 2000).

A simple examination of the bathymetric map and topographic maps of Karpathos and Kasos reveals two distinct directions in the morphology. The northern and central parts of Karpathos show a N-S direction, while the southern parts of Karpathos and Kasos exhibit a NW-SE direction (Athanassiadis, 2000).

In the islet of Armathia and at Korakia, there is a small circular depression known as a sinkhole, formed through exokarstic processes in the limestone and dolomite of the 'breccia karst of Armathia.' This depression contains brackish water, is located near sea level, and is situated close to the coast. This suggests that tectonic movements, potentially vertical, during the Neogene and Quaternary periods caused the uplift of Karpathos and Kasos, leading to enhanced karstic weathering (Athanassiadis, 2000).

The present shape and overall morphology of the islands are influenced by neotectonic factors and lithological structure. Neotectonic factors include fault zones, individual faults, and vertical movements as a whole. Wave erosion, rainfall erosion, and watercourses have accentuated these tectonic and lithological lines, resulting in the characteristic erosional forms observed today (Athanassiadis, 2000).

Coastlines along rocky formations such as limestones, dolomites, marly limestones, and chalky marls are prevalent along the majority of Kasos' coastline. These coasts are typically steep and exhibit remnants of reflective surfaces and overall tectonic lines, indicating the factors contributing to the formation of these islands. In Kasos and the nearby islets, the prevailing coasts have directions ranging from northeast to southwest and from northwest to southeast (Athanassiadis, 2000).

The hydrographic network and watercourses have formed marine terraces, flat surfaces, and notches at specific moments along the entire length of Kasos' coasts, all at the same sea level. The elevation of each feature reflects the magnitude and direction of vertical movements, while the observed elevation differences in various locations express the form and scale of tectonic deformations resulting from successive activations of intermediate faults after their formation (Athanassiadis, 2000).

4.3 Seismology of Kasos island

The seismological activity of Kasos Island has been studied through historical seismic data, providing valuable insights into its earthquake occurrences. Notably, between the years 1956 and 1986, the island experienced three earthquakes that resulted in catastrophic damage, while four earthquakes were felt in both Karpathos and Kasos. Interestingly, six out of the seven recorded earthquakes took place from 1926 to 1986, raising questions about the lack of evidence for seismic disasters in Karpathos and Kasos during the historical period from 550 BC to 1956 AD. It is worth noting that within this historical timeframe, the region surrounding these islands experienced numerous strong earthquakes with a magnitude of M>=6 R, which, surprisingly, did not cause damage to Karpathos and Kasos (Athanassiadis, 2000).

Prior to the mid-20th century, damages and catastrophes in Karpathos and Kasos mostly originated from distant earthquakes, particularly those occurring near Rhodes. However, several notable earthquakes directly affecting Kasos Island are worth mentioning. The first significant event took place on October 12, 1856, at 02:45, with coordinates 35.6° N and 26.0° E. This destructive earthquake, measuring M=8.2,

primarily impacted Crete, Kasos, Karpathos, Rhodes, Santorini, and Amorgos. In Kasos, three villages were completely destroyed (Athanassiadis, 2000).

Another impactful earthquake occurred on June 26, 1926, at 19:46:34, with coordinates 36.5° N and 27.5° E. Originating from Rhodes, this earthquake had a magnitude of M=8.0 (XI, Arhangelos) and resulted in significant damage to houses in Karpathos, Kasos, Kastellorizo, and Kos (Athanassiadis, 2000).

On February 9, 1948, at 12:58:13, an earthquake with coordinates 35.5° N and 27.2° E struck Karpathos with a magnitude of M=7.1 (IX, Karpathos). The quake caused damage in Poli, Kasos, with subsequent aftershocks leading to further damage in Karpathos and Kasos. The largest aftershock occurred on March 29, measuring M=5.6 (Athanassiadis, 2000).

Another notable event is the earthquake that took place on June 30, 1958, at 08:42:44, with coordinates 36.4° N and 27.3° E. This earthquake with a magnitude of M=6.0 (V) was strongly felt in Symi and Rhodes and also affected Samos, Kos, Kalymnos, Rethymno, Kasos, Karpathos, and Kastellorizo (Athanassiadis, 2000).

5. Marine terraces in Kasos island

Marine terraces in Kasos Island offer valuable insights into the geological history and tectonic activity of the region. These terraces, belonging to the marine Upper Quaternary period, consist of hard and cohesive coarse-grained calcarenites, biocalcarenites, and cobblestones. They represent purely coastal deposits, with thickness ranging from 1-2 meters to 6-7 meters, and are found at elevations ranging from sea level to 120 meters. The age of these terraces has been determined through the identification of characteristic gastropod fossils, such as Strombus bubonius L.K. and Conus testudinarius MAPTINI, indicating a Tyrrhenian age (Athanassiadis, 2000).

In Kasos Island and the nearby islet of Armathia, specific formations have been observed. Platy Avlaki bay in Kasos Island hosts limestone terrace deposits, approximately 4-5 meters thick, at an altitude of 10-15 meters. On the islets of Armathia and Makronisi, a large Tyrrhenian terrace with the presence of Strombus bubonius L.K. and Conus testudinarius MAPTINI has been identified at an altitude of 20-30 meters. Although radio dating is absent, based on its similarity in thickness and rich Tyrrhenian macrofauna to the large terrace in the Ag. Ioannis basin, this terrace is estimated to be around 260,000 years old (Athanassiadis, 2000).

To establish the relative age of these terraces and fossilized shorelines, they correlated them with various lower and upper Pleistocene terraces found at different elevations. In the Mesochori area, Calabrian terraces at 400 meters and 300 meters elevation in Exovouno and Rokli, as well as Tyrrhenian and upper Pleistocene terraces in Leuko, Ammopi, and Kastello, have been identified. Additionally, the absence of marine sediments from post-Eastern Miocene to pre-Tyrrhenian periods in Kasos and Armathia suggests that these islands remained emergent for the majority of their existence from the Upper Miocene to the present era. The presence of submerged aeolianites beneath the current sea level further supports the notion that the low coast around Fry sank at some point, although the specific age is not specified (Athanassiadis, 2000).

In conclusion, the formation age of the planation surfaces and paleo-shorelines in Karpathos and Kasos is determined to be younger than the Lower Pliocene. The geological evidence suggests that these surfaces and shorelines were formed during the Upper Pliocene and Pleistocene periods, characterized by vertical tectonic movements causing gradual uplift of the two islands (Athanassiadis, 2000). By studying the marine terraces and their ages, we gain a better understanding of the geological processes and tectonic history of Kasos Island.

5.1 Mapping marine terraces on Kasos Island

The mapping process of the marine terraces on Kasos Island involved a comprehensive analysis using Geographic Information System (GIS) with a digital elevation model (DEM) file in a scale of 1:50000. Through the utilization of GIS technology and examination of images, seven pairs of marine terraces were identified and mapped across various regions of the island. Each pair of terraces represents distinct elevations and locations, providing valuable insights into the geological history of Kasos.

The first pair, T1, is situated at an elevation of 0-20 meters and can be found in the southern and western areas of Kasos Island, specifically in the Armathia islet. Moving to an elevation of 20-40 meters, T2 emerges in the northern region of Agios Ioannis, extending westward to Fry, encompassing the entirety of Makronisi, and stretching into the southern part of Kasos Island. According to Athanassiadis, (2000), T2 corresponds to the Tyrrhenian terrace, estimated to be approximately 260,000 years old. This terrace is characterized by the presence of significant gastropod fossils such as Strombus bubonius L.K. and Conus testudinarius MAPTINI.

Continuing the mapping process, T3 is encountered at an elevation of 20-40 meters, prominently observed in the Agios Ioannis region, as well as in the Arvanitochori and Poli regions, along with their surrounding areas. As we ascend to an elevation of 40-60 meters, T4 comes into view, occupying the high terrace position in Armathia islet, extending towards the western regions of Arvanitochori and Poli, and further encompassing Agia Marina and the eastern part of Antiperatos.

Moving higher to an elevation of 60-80 meters, T5 emerges in the Agia Marina and Arvanitochori regions, providing an elevated perspective of the island's geological formations. As we ascend to an elevation of 80-100 meters, T6 comes into view. Finally, at an elevation of 100-120 meters, T7 becomes apparent in the southern parts of Agia Marina and Arvanitochori, offering a panoramic view of the island's geological features.

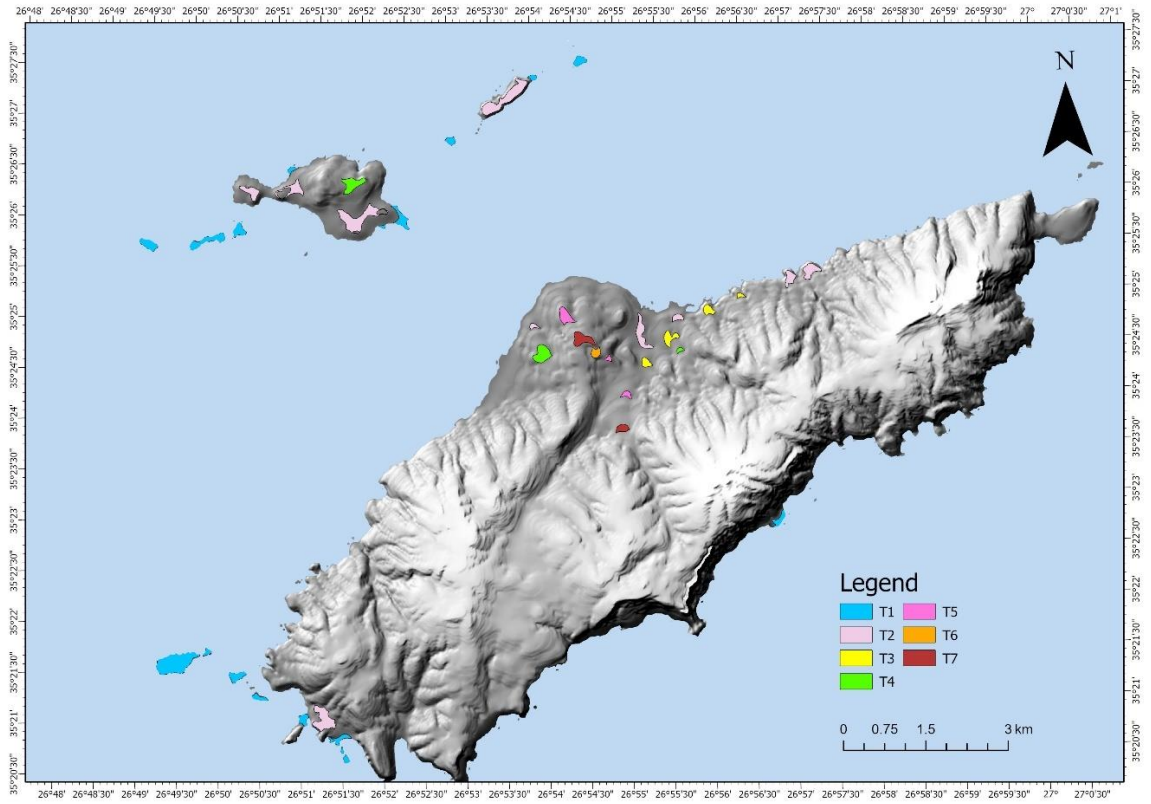

Figure 18 *Marine terraces in Kasos island and in Kasonisia.*

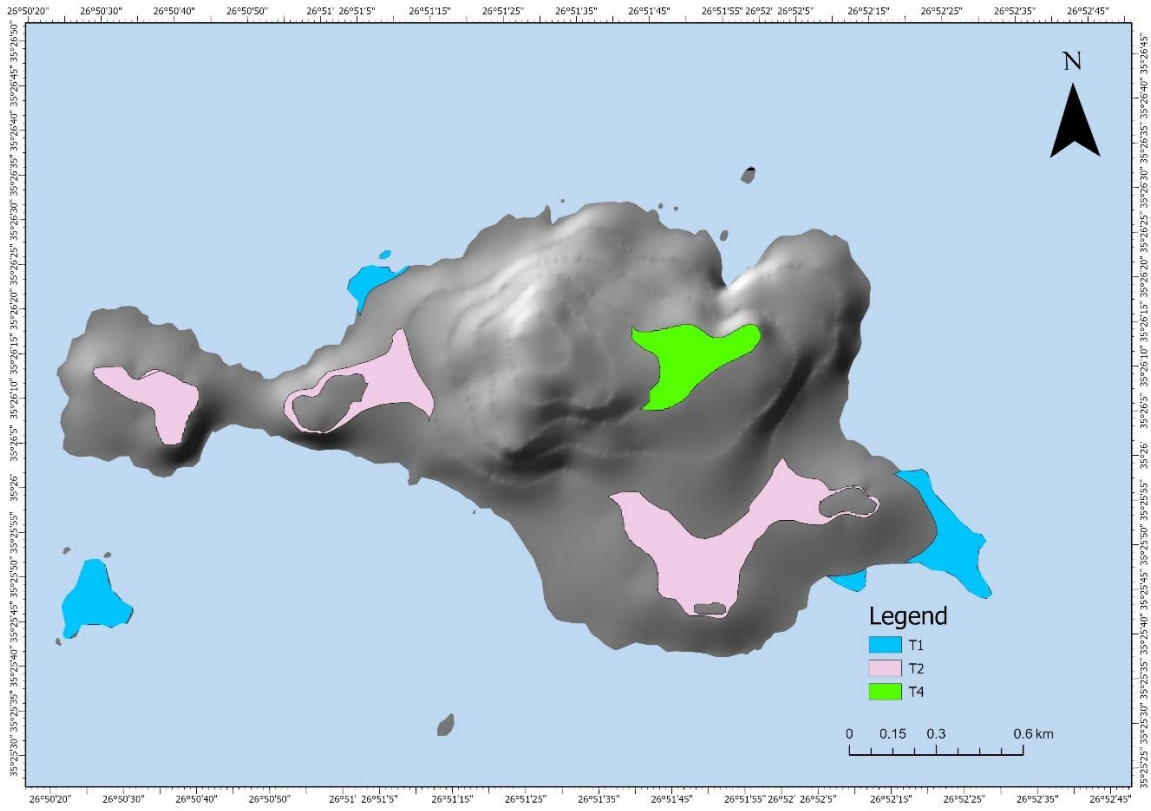

Figure 19 *Marine terraces in Armathia island.*

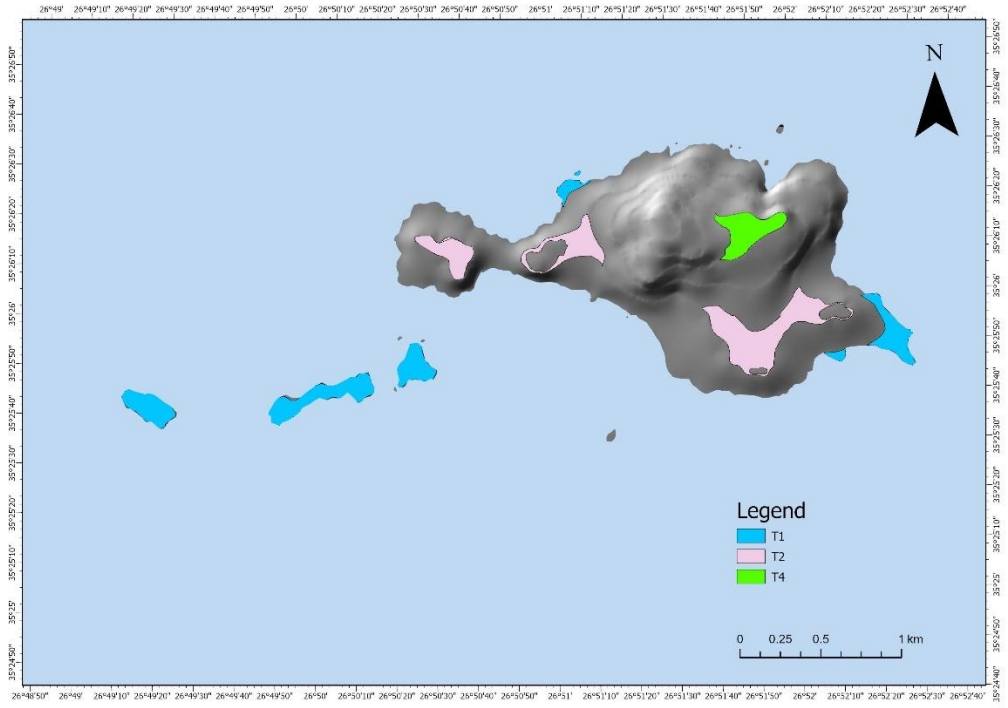

Figure 20 *Marine terraces in Armathia island and its islets.*

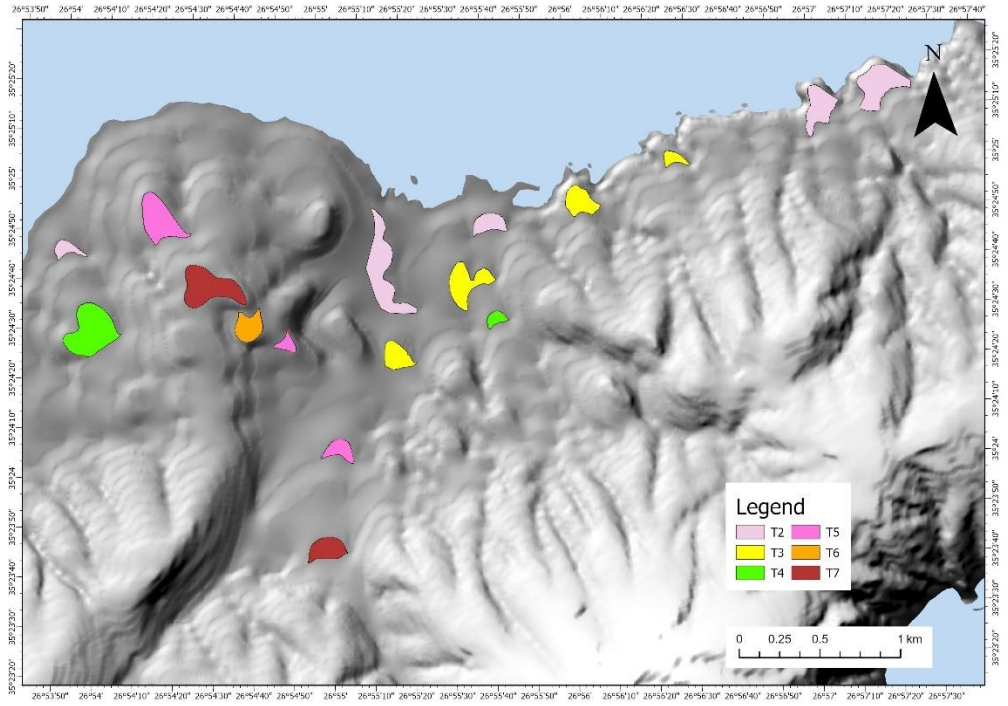

Figure 21 *Marine terraces in Chora of Kasos and its surrounding areas.*

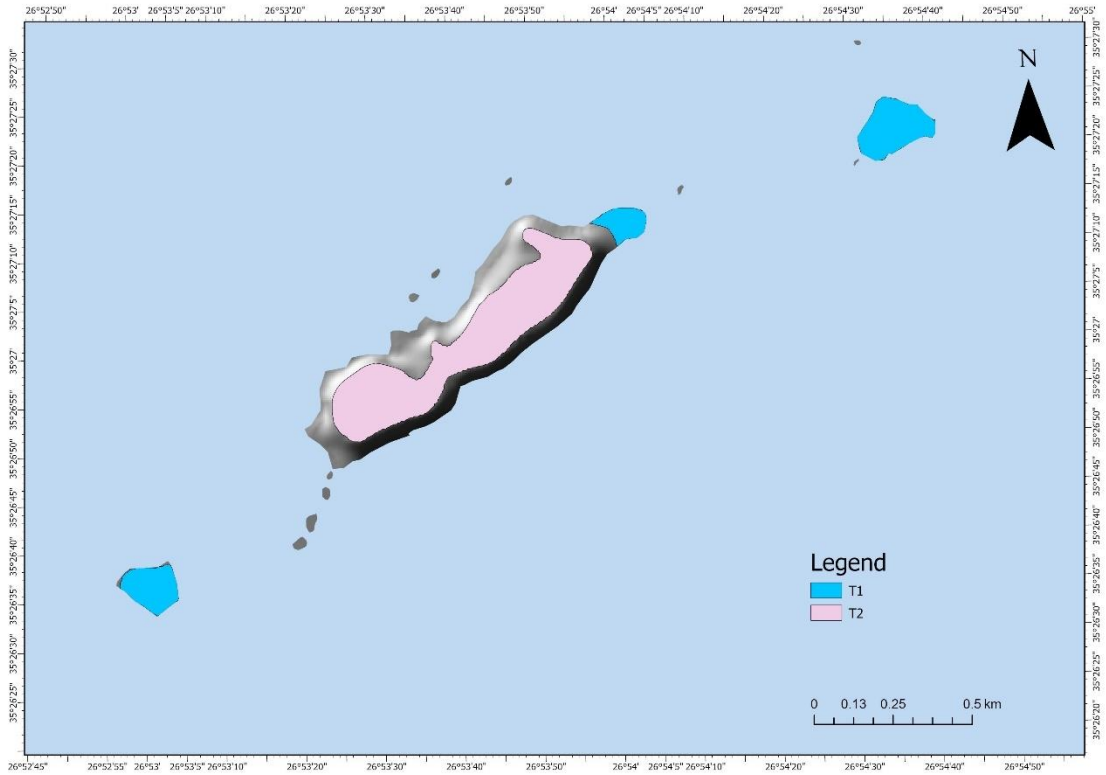

Figure 22 *Marine terraces in Porioni and Makronisi islands.*

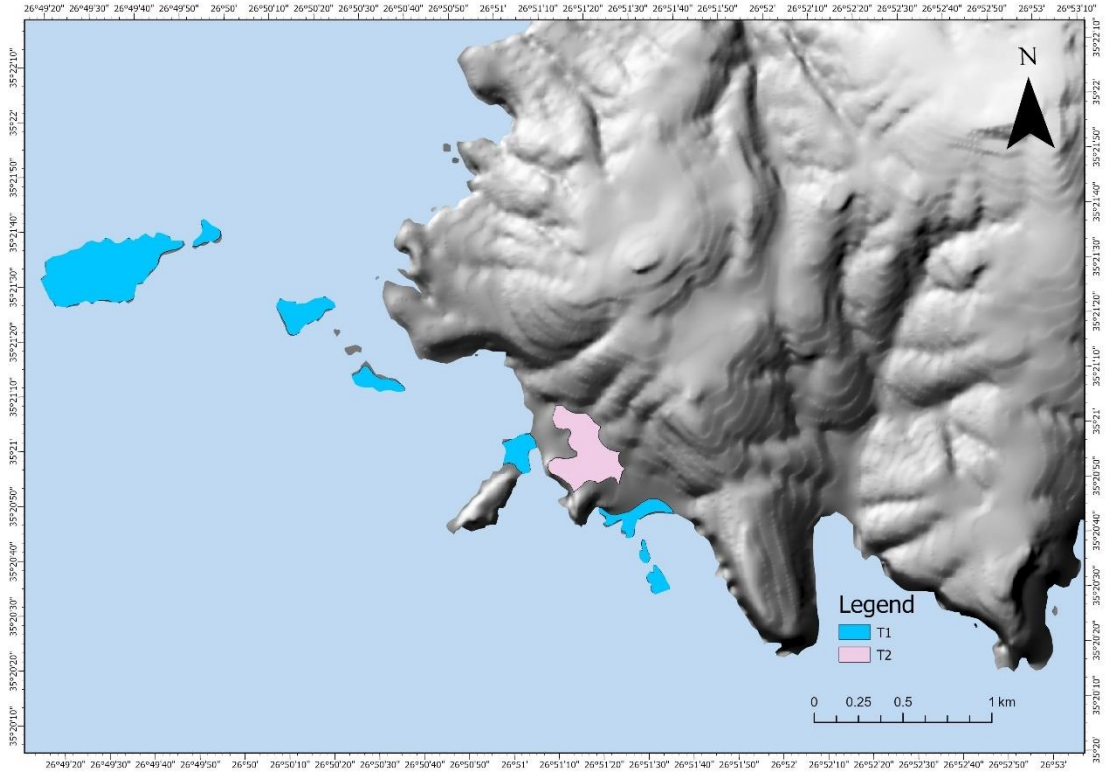

Figure 23 *Marine terraces in the southern part of Kasos island.*

6. Results and conclusions

The comparison of the pairs of marine terraces located on different parts of Kasos Island and on neighboring islands provides valuable insights into the island's tectonic history and the effects of sea level changes. The presence or absence of these terraces can indicate the relative uplift or subsidence of the landmasses over time.

In Kasos Island, we have identified seven pairs of marine terraces: T1, T2, T3, T4, T5, T6 and T7, each occurring at different elevations. These terraces represent distinct periods of tectonic activity or fluctuations in sea level. The mapping process using GIS technology and the analysis of the DEM files have allowed us to visualize and study these terraces in detail.

Comparing the pairs of terraces located on Kasos Island itself, we can observe variations in their elevations and distribution across different regions. For example, T1 is found at an elevation of 0m and is primarily located in the south and west of Kasos Island, while T2 is situated at an elevation of 20-40m and is present in the northern part of Agios Ioannis region, west of Fry, as well as in Armathia islet and Makronisi. Similarly, T3, T4, T5, T6 and T7 occur at higher elevations, reflecting successive tectonic events or changes in sea level.

When comparing the terraces on Kasos Island with those on lower islands such as Armathia, an intriguing pattern emerges. The absence of certain terrace pairs on Kasos Island suggests that either they have been eroded over time, leaving only remnants on mountain tops, or these lower islands were once underwater during the formation of those particular terraces. This discrepancy in terrace presence and elevation can be attributed to variations in tectonic activity and subsidence rates between different parts of the region.

The tectonic movements responsible for the formation of marine terraces on Kasos Island and the neighboring islands are complex and multifaceted. It is likely that both vertical uplift and subsidence have played significant roles in shaping the landscape over geological timescales. The marine terraces serve as important indicators of past tectonic events and sea level changes, providing a valuable record of the island's geological history.

In conclusion, the comparison of marine terraces across Kasos Island and neighboring islands highlights the interplay between tectonic processes and sea level fluctuations. The absence of certain terrace pairs on Kasos Island suggests erosion or past submergence of lower islands, while the presence of others indicates tectonic uplift or differential subsidence. These findings underscore the significance of marine terraces as valuable markers for understanding tectonic activity and past environmental conditions in the region. Further research and investigation are necessary to unravel the intricate geological processes that have shaped the marine terraces of Kasos Island and surrounding areas.

Marine terraces are coastal landforms that owe their creation to the combination of eustatic and tectonic processes. The study of these landforms contributes to the recognition of eustatic changes and tectonics, since each terrace created represents a tectonic event or change in sea level. Hence, their study is very important and fundamental in Quaternary stratigraphy (Evelpidou, 2020).

7. References

Angelier, J., Lybéris, N., Le Pichon, X., Barrier, E., & Huchon, P. (1982). The tectonic development of the hellenic arc and the sea of crete: A synthesis. *Tectonophysics*, *86*(1–3). https://doi.org/10.1016/0040-1951(82)90066-X

Athanassas, C., & Fountoulis, I. (2013). Quaternary neotectonic configuration of the southwestern Peloponnese, Greece, based on luminescence ages of marine terraces. *Journal of Earth Science*, *24*(3), 410–427. https://doi.org/10.1007/s12583-013-0334-1

Athanassiadis, D. (2000). *Neotectonic and seismotectonic studies on the Karpathos-Kassos islands and their wider area*. National Technical University of Athens.

Bilbao-Lasa, P., Jara-Muñoz, J., Pedoja, K., Álvarez, I., Aranburu, A., Iriarte, E., & Galparsoro, I. (2020). Submerged Marine Terraces Identification and an Approach for Numerical Modeling the Sequence Formation in the Bay of Biscay (Northeastern Iberian Peninsula). *Frontiers in Earth Science*, *8*(March), 1–20. https://doi.org/10.3389/feart.2020.00047

Cattaneo, C., & Grano, M. (2021). Kasos : an unexpected island . Floristic and ecological analysis of Kasos Island (SE Aegean , Dodecanese , Greece), with noteworthy floristic additions. *Phytologia Balcanica*, *27*(3), 345–371.

Cerrone, C., Di Donato, V., Mazzoli, S., Robustelli, G., Soligo, M., Tuccimei, P., & Ascione, A. (2021). Development and deformation of marine terraces: Constraints to the evolution of the Campania Plain Quaternary coastal basin (Italy). *Geomorphology*, *385*, 107725. https://doi.org/10.1016/j.geomorph.2021.107725

Dermitzakis, M. D., & Triantaphyllou, M. V. (1990). Contribution to the Stratigraphy of Miocene Sediments of Kassos island (South Sporades). *5th Congress*, 11.

Doutsos, T., & Kokkalas, S. (2001). Stress and deformation patterns in the Aegean region. *Journal of Structural Geology*, *23*(2–3), 455–472. https://doi.org/10.1016/S0191-8141(00)00119-X

Evelpidou, N. (2020). *Sea level Changes*. Da Vinci, Athens.

Gaki-Papanastassiou, K., Karymbalis, E., Papanastassiou, D., & Maroukian, H. (2009). Quaternary marine terraces as indicators of neotectonic activity of the Ierapetra normal fault SE Crete (Greece). *Geomorphology*, *104*(1–2), 38–46. https://doi.org/10.1016/j.geomorph.2008.05.037

Geological Survey of Greece. (2022). *Geology Map 1:500.000*. https://gaia.igme.gr/portal/home/item.html?id=61dc7b67790944a198d4dbdc876d1a3c

González-Acebrón, L., Mas, R., Arribas, J., Gutiérrez-Mas, J. M., & Pérez-Garrido, C. (2016). Very coarse-grained beaches as a response to generalized sea level drops in a complex active tectonic setting: Pleistocene marine terraces at the Cadiz coast, SW Spain. *Marine Geology*, *382*, 92–110. https://doi.org/10.1016/j.margeo.2016.09.007

Granger, D. E., & Riebe, C. S. (2014). Cosmogenic Nuclides in Weathering and Erosion. *Treatise on Geochemistry: Second Edition*, *7*, 401–436. https://doi.org/10.1016/B978-0-08-095975-7.00514-3

Gurrola, L. D., Keller, E. A., Chen, J. H., Owen, L. A., & Spencer, J. Q. (2014). Tectonic geomorphology of marine terraces: Santa Barbara fold belt, California. *Bulletin of the Geological Society of America*, *126*(1–2), 219–233. https://doi.org/10.1130/B30211.1

Howell, A., Jackson, J., England, P., Higham, T., & Synolakis, C. (2015). Late Holocene uplift of Rhodes, Greece: Evidence for a large tsunamigenic

earthquake and the implications for the tectonics of the eastern Hellenic Trench System. *Geophysical Journal International*, *203*(1), 459–474. https://doi.org/10.1093/gji/ggv307

Karymbalis, E., Tsanakas, K., Tsodoulos, I., Gaki-Papanastassiou, K., Papanastassiou, D., Batzakis, D. V., & Stamoulis, K. (2022). Late Quaternary Marine Terraces and Tectonic Uplift Rates of the Broader Neapolis Area (SE Peloponnese, Greece). *Journal of Marine Science and Engineering*, *10*(1). https://doi.org/10.3390/jmse10010099

Kim, K. J., & Sutherland, R. (2004). Uplift rate and landscape development in southwest Fiordland, New Zealand, determined using 10Be and 26Al exposure dating of marine terraces. *Geochimica et Cosmochimica Acta*, *68*(10), 2313–2319. https://doi.org/10.1016/j.gca.2003.11.005

Kokkalas, S., & Doutsos, T. (2001). Strain-dependent stress field and plate motions in the south-east Aegean region. *Journal of Geodynamics*, *32*(3), 311–332. https://doi.org/10.1016/S0264-3707(01)00035-7

Kondo, H., & Owen, L. A. (2013). 5.12 Paleoseismology. *Treatise on Geomorphology*, *5*, 267–299. https://doi.org/10.1016/B978-0-12-374739-6.00092-0

Kondo, Hisao, Owen, L. A., & Figueiredo, P. M. (2022). Paleoseismological Studies. *Treatise on Geomorphology*, 495–562. https://doi.org/10.1016/B978-0-12-818234-5.00156-5

Mascle, J., Cleac'h, A. Le, & Jongsma, D. (1986). The eastern Hellenic margin from Crete to Rhodes: Example of progressive collision. *Marine Geology*, *73*(1–2), 145–168. https://doi.org/10.1016/0025-3227(86)90116-7

Mastropavlos, G. (2019). *KASOS: MONUMENTAL TOPOGRAPHY AND CERAMIC FINDS FROM GEOMETRIC TO HELLENISTIC PERIODS*. Aristotle University of Thessaloniki.

May, V. (1993). *Marine terraces*. *9*, 632–633.

Melas, E. (1984). *The islands of Karpathos, Saros and Kassos in the Neolithic and Bronze Ages*. University of London.

Nandy, S., Taloor, A. K., & Chandra Kothyari, G. (2021). Mapping of major river terraces and assessment of their characteristics in Upper Pindar River Basin, Uttarakhand: A geospatial approach. *Quaternary Science Advances*, *4*, 100032. https://doi.org/10.1016/j.qsa.2021.100032

Pirazzoli, P. A. (2013). SEA LEVEL STUDIES | Geomorphological Indicators. *Encyclopedia of Quaternary Science: Second Edition*, 377–384. https://doi.org/10.1016/B978-0-444-53643-3.00133-3

Racano, S., Jara-Muñoz, J., Cosentino, D., & Melnick, D. (2020). Variable Quaternary Uplift Along the Southern Margin of the Central Anatolian Plateau Inferred From Modeling Marine Terrace Sequences. In *Tectonics* (Vol. 39, Issue 12). https://doi.org/10.1029/2019TC005921

Ricchi, A., Quartau, R., Ramalho, R. S., Romagnoli, C., Casalbore, D., Ventura da Cruz, J., Fradique, C., & Vinhas, A. (2018). Marine terrace development on reefless volcanic islands: New insights from high-resolution marine geophysical data offshore Santa Maria Island (Azores Archipelago). *Marine Geology*, *406*(May), 42–56. https://doi.org/10.1016/j.margeo.2018.09.002

Rovere, A., Raymo, M. E., Vacchi, M., Lorscheid, T., Stocchi, P., Gómez-Pujol, L., Harris, D. L., Casella, E., O'Leary, M. J., & Hearty, P. J. (2016). The analysis of Last Interglacial (MIS 5e) relative sea-level indicators: Reconstructing sea-level in a warmer world. *Earth-Science Reviews*, *159*, 404–427.

https://doi.org/10.1016/j.earscirev.2016.06.006
Tanaka, K., Hataya, R., Spooner, N. A., Questiaux, D. G., Saito, Y., & Hashimoto, T. (1997). Dating of marine terrace sediments by ESR, TL and OSL methods and their applicabilities. *Quaternary Science Reviews*, *16*(96), 257–264. https://doi.org/10.1016/S0277-3791(96)00092-3
Trenhaile, A. S. Ã. (2002). Modeling the development of marine terraces on tectonically mobile rock coasts. *Marine Geology*, *185*(3–4), 341–361. https://doi.org/10.1016/S0025-3227(02)00187-1
Tsanakas, K., Saitis, G., Evelpidou, N., Karymbalis, E., & Karkani, A. (2022). Late Pleistocene Geomorphic Evolution of Cephalonia Island , Western Greece , Inferred from Uplifted Marine Terraces. *Quaternary*, *5*(35). https://doi.org/10.3390/ quat5030035
Wegmann, K. W., & Gallen, S. F. (2022). Tectonic Geomorphology Above Mediterranean Subduction Zones. *Treatise on Geomorphology*, 87–119. https://doi.org/10.1016/B978-0-12-818234-5.00223-6
Zazo, C. (1999). Interglacial sea levels. *Quaternary International*, *55*(1), 101–113. https://doi.org/10.1016/S1040-6182(98)00031-7